JOC Article
pubs.acs.org/joc

Synthesis and Characterization of Fluorinated Heterofluorene-Containing Donor−Acceptor Systems

Katharine Geramita,[†] Yuefei Tao,[‡] Rachel A. Segalman,[‡] and T. Don Tilley*,[†]

[†]*Department of Chemistry and* [‡]*Department of Chemical Engineering, University of California at Berkeley, Berkeley California 94720*

tdtilley@berkeley.edu

Received December 7, 2009

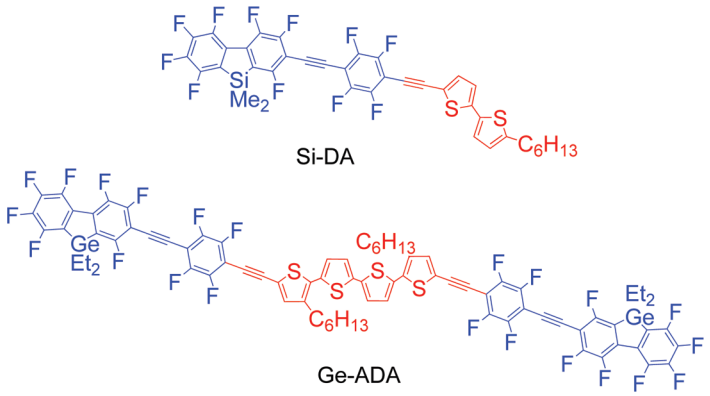

A series of oligothiophene-perfluoro-9-heterofluorene donor−acceptor (DA) compounds was synthesized via a combination of nucleophilic aromatic substitution (S_NAr_F) and palladium coupling reactions. These compounds are of interest as possible building blocks for materials with useful electron transport properties, since they possess relatively low LUMO energy levels of −3.3 to −3.6 eV (as determined by differential pulse voltammetry). The HOMO−LUMO energy gaps, as determined by UV−vis spectroscopy, range between 2.4 and 2.5 eV, and photoluminescence emission spectra reveal λ_{ems} values in the range of 480−600 nm (corresponding to yellow−orange emission). Dilute solution-state photoluminescence quantum yields were significantly lower than those of the pure acceptor heterofluorenes (0.02−0.38 for the DA compounds vs ∼1 for the pure acceptors), and notable solvatochromism in the fluorescence suggests emission from a charge-separated state. Theoretical calculations show that HOMO-level electron density is more localized on the thiophene fragment, while the LUMO level electron density is mostly associated with the electron-deficient portion of the molecule. Photovoltaic (PV) devices based on DA/poly-3-hexylthiophene (P3HT) blends exhibit improved performance over P3HT-only devices, suggesting the ability of these DA compounds to transport electrons in the solid state.

Introduction

The use of organic semiconducting materials for applications in "plastic electronics", such as field effect transistors (FETs), organic light emitting diodes (OLEDs) and photovoltaics (PVs), continues to attract considerable interest.[1] Organic systems offer the possibility for cheap raw materials and low processing costs and can be tailored to access a wide range of physical, optical, and electrical properties.[1−4]

(1) (a) Forrest, S. R. *Chem. Rev.* **1997**, *97*, 1793. (b) Jenekhe, S. *Chem. Mater.* **2004**, *16*, 4382 (special issue on organic electronics). (c) Forrest, S. R.; Thompson, M. E. *Chem. Rev.* **2007**, *107*, 923 (special issue on organic electronics).

(2) Hwang, D. H.; Kim, S. K.; Park, M. J.; Koo, B. W.; Kang, I. N.; Kim, S. H.; Zyung, T. *Chem. Mater.* **2004**, *16*, 1298.

(3) Schwartz, M; Srinivas, G; Yeates, A.; Berry, R.; Dudia, D. *Synth. Met.* **2004**, *143*, 229.

(4) Zhu, Y.; Alam, M. M.; Jenekhe, S. A. *Macromolecules* **2003**, *36*, 8958.

DOI: 10.1021/jo902488w Published on Web 03/02/2010

Within this context, investigations have targeted conjugated oligomers and polymers that are electron-rich (donor) or electron-poor (acceptor) in character. Fully conjugated donor−acceptor systems, D-π-A, that incorporate both electron-rich and electron-poor segments, are particularly attractive for their ambipolar charge injection (electrons and holes) and transport properties. These systems are of interest for a variety of electronic applications for which balancing the transport properties of both holes and electrons is important (OLEDs, PVs, etc.).[5] Conjugated D-π-A systems are promising new materials for photonic applications (two-photon absorption, all optical computing, signal processing, etc.), since their inherent dipole enhances the nonlinear optical response properties for the molecule.[6,7] Finally, the development of low band gap materials (organic PVs and conductors) in which intramolecular charge transfer between donor and acceptor fragments advantageously perturbs the HOMO and LUMO energy levels has progressed as new D-π-A systems have become available.[8]

Generally, conjugated organic π-systems that behave as electron-donating, hole-transporting (p-type) materials are readily available;[9] however, organic compounds that exhibit efficient electron-accepting, electron-conducting (n-type) properties are much less developed.[4,10] Useful n-type organic materials possess a low barrier to electron injection and effectively transport a negative charge. While it is generally accepted that a low-energy LUMO should facilitate charge injection, the attributes that contribute to high electron mobility are not well understood and include the nature and length of the conjugated π-system, the strength of intermolecular interactions, and various elements of device construction (including surface passivation, assembly techniques and processing conditions).[5,11] Electron-deficient π-systems are thought to be associated with high electron mobility, and pyridines, oxadiazoles, perylene diimides, metalloles and fluorinated aromatics have been identified as potential n-type materials.[12−17] Additionally, close cofacial intermolecular packing has been associated with increased charge transport in a number of organic systems.[9] Therefore, molecular organic building blocks that contain an electron-deficient, extended π-system, a stabilized LUMO, and close cofacial stacking in the solid state would be of great interest to the development of this field.

Metalloles (**A**), which are five-membered heterocycles containing a heteroatom and a diene moiety, represent a potentially large class of compounds of particular interest to organic electronic materials research, since their structures should be readily modified to independently alter electronic and physical properties. Metalloles are associated with low energy LUMO levels, resulting from stabilization of the diene π-system via interaction with the heteroatom based σ^* oribtals.[18,19] The LUMO energy level is generally unaffected by minor variations in the R groups on the heteroatom,[20,21] which can be tuned to modify solubility and packing properties. Siloles (**A**, E = Si) in particular have exhibited exceptionally good performance in OLED devices, and relatively high electron mobilities have been measured.[14a,22] Crystal structures of many silole-based materials have revealed poor intermolecular cofacial interactions due to orientation of the aryl groups that usually occupy the 3- and 4-positions (in many cases a requirement for the silole synthesis), and this limits their suitability for applications in which cofacial packing of aromatic systems is important.[14a,22]

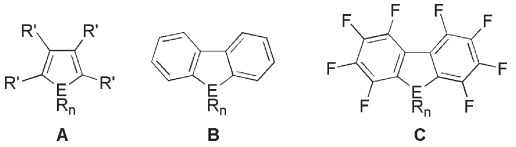

Main group compounds containing the dibenzometallole (or metallofluorene) (**B**; E = Si, Ge, Sn, etc.) fragment are interesting candidates for n-type materials, since they possess a planar aromatic structure while maintaining the LUMO-lowering ability of the metallole fragment. In general, fluorene-based systems are electron-rich, tend to pack in a herringbone structure, and do not exhibit the desired cofacial interactions.[23−25] However, fluorine atom substituents in the aromatic system may improve both electron transport and cofacial packing. The highly electronegative nature of the fluorine substituent draws electron density

(5) Zaumseil, J.; Sirringhaus, H. *Chem. Rev.* **2007**, *107*, 1296.
(6) (a) Albota, M.; Beljonne, D.; Breda, J.-L.; Ehrlich, J.; Fu, J.-Y.; Heikal, A.; Hess, S.; Kogej, T.; Levin, M.; Marder, S.; McCord-Maughon, D.; Perry, J.; Rockel, H.; Rumi, M.; Subramanium, G.; Webb, W.; Wu, X.-L.; Xu, C. *Science* **1998**, *281*, 1653. (b) He, G.; Tan, L.-S.; Zheny, Q.; Prasad, P. *Chem. Rev.* **2008**, *108*, 1245.
(7) (a) Day, P. N.; Nguyen, K. A.; Pachter, R. *J. Phys. Chem. B* **2005**, *109*, 1803. (b) Reinhardt, B. A.; Brott, L. L.; Clarson, S. J.; Dillard, A. G.; Bhatt, J. C.; Kannan, R.; Yuan, L.; He, G. S.; Prasad, P. N. *Chem. Mater.* **1998**, *10*, 18.
(8) (a) Pappenfus, T. M.; Hermanson, B. J.; Helland, T. J.; Lee, G. G. W.; Drew, S. M.; Mann, K. R.; McGee, K. A.; Rasmussen, S. C. *Org. Lett.* **2008**, *10*, 1553. (b) Bendikov, M.; Wudl, F.; Perepichka, D. F. *Chem. Rev.* **2004**, *104*, 4891.
(9) Hutchison, G.; Ratner, M.; Marks, T. J. *J. Am. Chem. Soc.* **2005**, *127*, 16866.
(10) Tonzola, C. J.; Alam, M. M.; Kaminsky, W.; Jenekhe, S. A. *J. Am. Chem. Soc.* **2003**, *125*, 13548.
(11) (a) Chua, L.-L.; Zaumseil, J.; Chang, J.-F.; Ou, E.; Ho, P.; Sirringhaus, H.; Friend, R. *Nature* **2005**, *434*, 194.
(12) Kulkarni, A.; Tonzola, C.; Babel, A.; Jenekhe, S. *Chem. Mater.* **2004**, *16*, 4556.
(13) Babudri, F.; Farinola, G.; Naso, F.; Ragni, R. *Chem. Commun.* **2007**, *10*, 1003.
(14) (a) Geramita, K.; McBee, J.; Shen, Y.; Radu, N.; Tilley, T. D. *Chem. Mater.* **2006**, *18*, 3261. (b) Tannaci, J. F.; Noji, M.; McBee, J.; Tilley, T. D. *J. Org. Chem.* **2007**, *72*, 5567.
(15) Tamao, K.; Uchinda, M.; Izumizawa, T.; Furukawa, K.; Yamaguchi, S. *J. Am. Chem. Soc.* **1996**, *118*, 11974.
(16) Facchetti, A.; Yoon, M. H.; Stern, C. L.; Katz, H. E.; Marks, T. J. *Angew. Chem., Int. Ed.* **2003**, *42*, 3900.
(17) Heidenhain, S. B.; Sakamoto, Y.; Suzuki, T.; Miura, A.; Fujikawa, H.; Mori, T.; Tokito, S.; Taga, T. *J. Am. Chem. Soc.* **2000**, *122*, 10240.
(18) (a) Tamao, K.; Yamaguchi, S.; Shiro, M. *J. Am. Chem. Soc.* **1994**, *116*, 11715. (b) Yamaguchi, S.; Tamao, K. *J. Chem. Soc., Dalton Trans.* **1998**, 3693.
(19) Hissler, M.; Dyer, P. W.; Reau, R. *Coord. Chem. Rev.* **2003**, *244*, 1.
(20) Geramita, K.; McBee, J.; Tilley, T. D. *J. Org. Chem.* **2009**, *74*, 820.
(21) Geramita, K.; McBee, J.; Tao, Y.; Segalman, R.; Tilley, T. D. *Chem. Commun.* **2008**, 5107.
(22) Murata, H.; Malliaras, G. G.; Uchida, M.; Shen, Y.; Kafafi, Z. H. *Chem. Phys. Lett.* **2001**, *339*, 161.
(23) (a) Rathnayake, H.; Cirpan, A.; Lahti, P.; Karasz, F. *J. Am. Chem. Soc.* **2006**, *18*, 560. (b) Heeney, M.; Bailey, C.; Giles, M.; Shkunov, M.; Sparrowe, D.; Tierney, S.; Zhang, W.; McCulloch, I. *Macromolecules* **2004**, *37*, 5250.
(24) Chen, C.-H.; Shen, W.-J.; Jakka, K.; Shu, C.-F. *Synth. Met.* **2004**, *143*, 215.
(25) Coropceanu, V.; Nakano, T.; Gruhn, N.; Kwon, O.; Yade, T.; Katsukawa, K.; Bredas, J.-L. *J. Phys. Chem. B* **2006**, *110*, 9482.

CHART 1

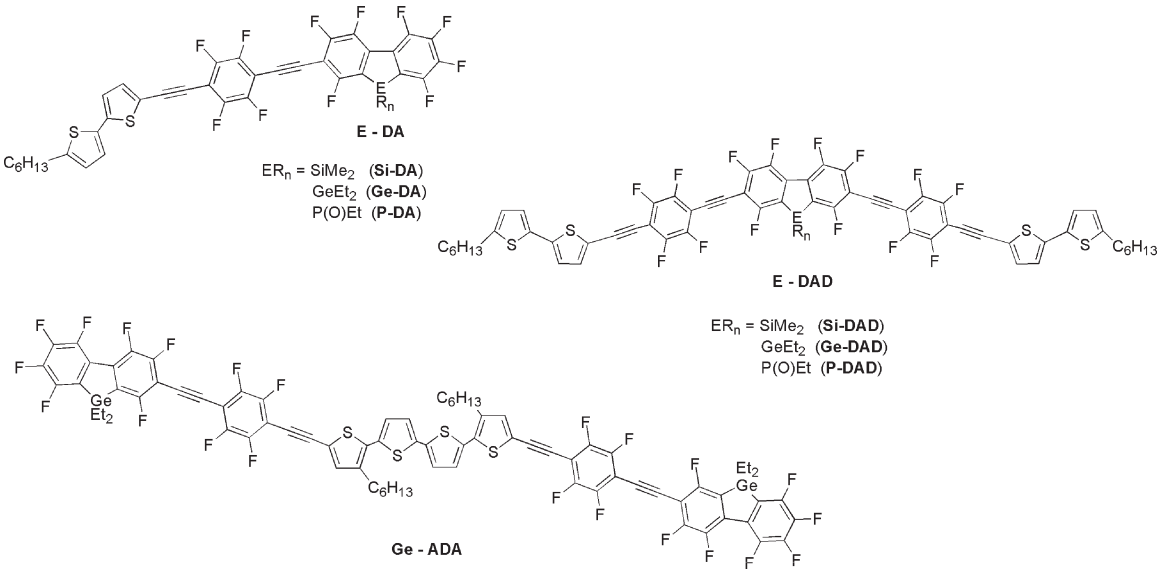

away from the aromatic π-system, rendering it electron-deficient and more suitable for electron accepting and transporting applications.[16,17,26] Additionally, highly fluorinated aromatic systems tend to pack cofacially, rather than in the herringbone motif observed for many nonfluorinated aromatic molecules.[27,28] Perfluorometallofluorenes (**C**) are a relatively unexplored class of molecules that combine these two elements of molecular design and should produce a series of molecules with low LUMO energies and electron-deficient π-systems that exhibit cofacial π-stacking in the solid state.

In addition to metalloles based on group 14 elements, the analogous phosphorus-based systems (phospholes) have shown great promise for a number of electronic applications.[19,29] Phospholes possess several interesting characteristics, including low aromatic character and $\sigma^*-\pi$ conjugation (similar to that observed for metalloles), which make them good candidates for organic electronic applications.[19,29] Phosphole-based systems have been shown to function as hole-transporting materials; however, the related phosphole oxide derivatives possess a more electron-deficient π-system. Thus the combination of PR or P(O)R groups with the highly electron-deficient perfluorofluorene framework should afford compounds with high electron affinities.[20,21]

The development of efficient organic photonic and electronic devices should benefit from the discovery of new electron-deficient materials that possess the desired physical and electronic characteristics. In pursuit of such compounds, this laboratory has developed a facile route to the 2,2′-dibromo-4,4′-diethynyl-3,3′,5,5′,6,6′-hexafluorobiphenyl moiety, which can easily be converted to a variety of 2,7-diethynyl functionalized heterofluorenes (eq 1).[21]

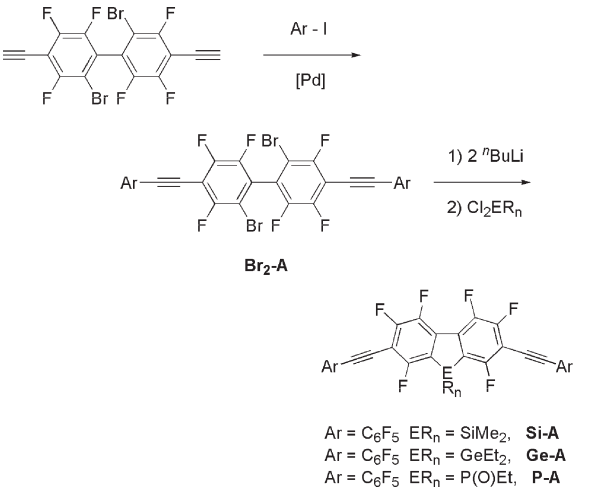

(1)

To date, poly- and oligothiophene derivatives are among the most efficient organic hole transport materials for PV and FET devices.[30] This is a direct result of the electron-rich nature of the thiophene ring and the ability of these rings to stack in a cofacial manner. These characteristics make oligothiophenes the ideal candidate for the donor fragment in the initial studies on perfluoroheterofluorene-containing, donor−acceptor (DA) compounds. In this report we describe the synthesis and optical and electrochemical characterization of a variety of thiophene-perfluoroheterofluorene DA compounds (Chart 1). The synthesis and characterization of these electron-deficient compounds provide a new series of organic donor−acceptor materials for evaluation in various applications.

(26) Facchetti, A.; Yoon, M.-H.; Stern, C. L.; Hutchison, G. R.; Ratner, M. A.; Marks, T. J. *J. Am. Chem. Soc.* **2004**, *126*, 13859.

(27) (a) Gierschner, J.; Ehni, M.; Egelhaaf, H.-J.; Medina, B. M.; Beljonne, D.; Benmansour, H.; Bazan, G. *J. Chem. Phys.* **2005**, *123*, 144914. (b) Cho, D.; Parkin, S.; Watson, M. *Org. Lett.* **2005**, *7*, 1067.

(28) Sakamoto, Y.; Komatsu, S.; Suzuki, T. *J. Am. Chem. Soc.* **2001**, *123*, 4643.

(29) Bumgartner, T.; Reau, R. *Chem. Rev.* **2006**, *106*, 4681.

(30) (a) Murphy, A. R.; Fréchet, J. M. *J. Chem. Rev.* **2007**, *107*, 1066. (b) Katz, H. E. *J. Mater. Chem.* **1997**, *7*, 369. (c) Garnier, F. *Pure Appl. Chem.* **1996**, *68*, 1455.

SCHEME 1

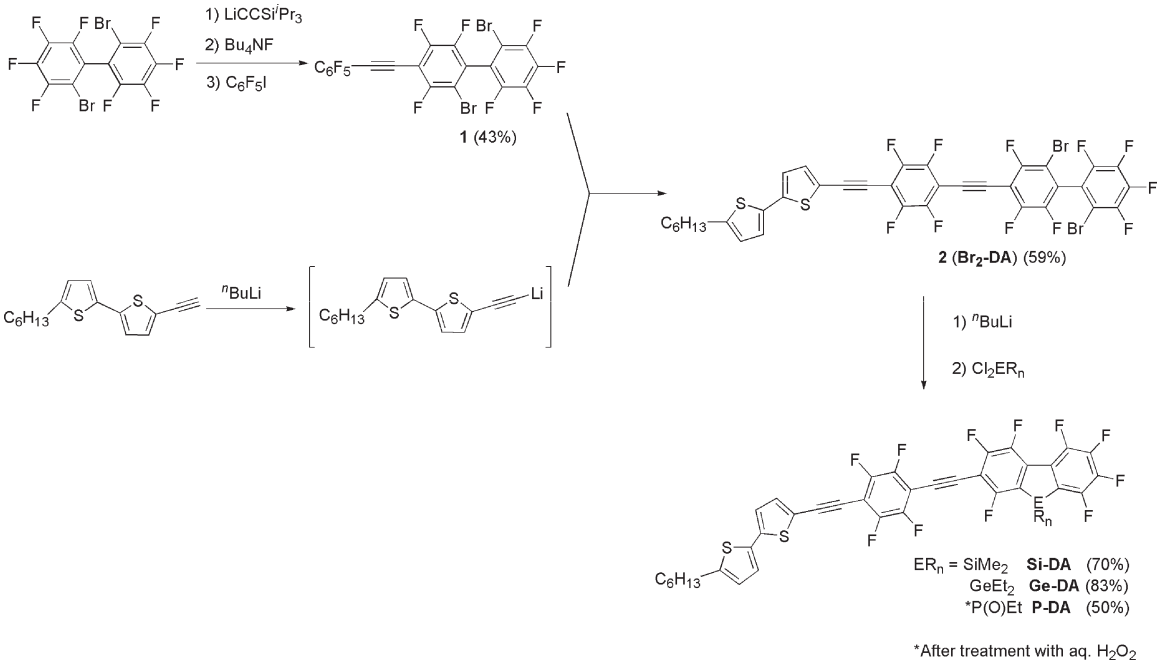

SCHEME 2

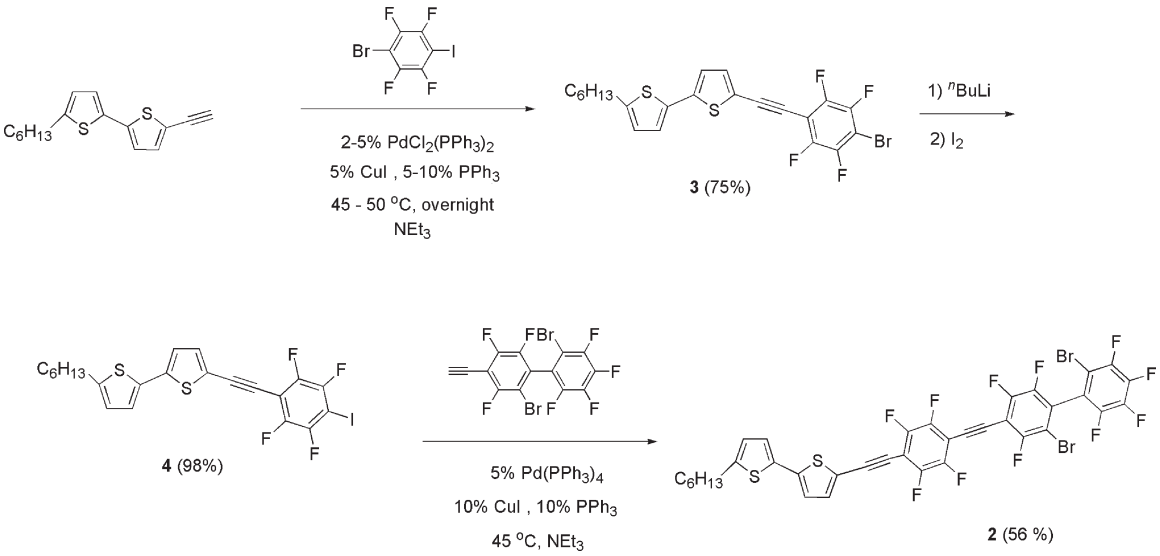

Results and Discussion

Synthesis of Donor−Acceptor Compounds. The synthesis of heptafluoroheterofluorene-based DA compounds is described in Schemes 1 and 2. The alkynyl functionality of **1** was installed via a nucleophilic aromatic substitution reaction of triisoproylsilyl lithium acetylide with 2,2′-dibromooctafluorobiphenyl under conditions similar to those described previously to prepare the dialkyne.[21] The triisopropylsilyl group was removed by addition of ^{n}Bu$_4$NF to a dilute (0.0001 M) toluene/THF solution (∼2% THF) of the 4-(triisopropylsilylethynyl)-2,2′-dibromo-3,3′,4′,5,5′,6,6′-heptafluorobiphenyl intermediate, and the unprotected diyne was then capped with C_6F_5 groups by an *in situ* Pd-catalyzed Sonagashira coupling reaction with C_6F_5I at 45 °C to give **1** in 43% yield based on the starting material 2, 2′-dibromooctafluorobiphenyl. The donor fragment, 2-ethynyl-2′-hexyl-5,5′-bithiophene, was synthesized by a Pd-catalyzed Sonagashira coupling reaction of 2-bromo-2′-hexyl-5,5′-bithiophene with ethynyltrimethylsilane, followed by trimethylsilyl deprotection with K_2CO_3 in a mixture of MeOH/THF/H_2O. Addition of 1 equiv of ^{n}BuLi to a THF solution of the donor alkyne produced the alkynyl lithium nucleophile *in situ*. The alkynyl lithium solution was then added to a solution of **1** in toluene at 0 °C to produce **2** (**Br$_2$-DA**) in moderate conversion (∼75% as determined by ^{19}F NMR). Compound **2** was isolated via column chromatography in 59% yield. Lithiation of **2** with ^{n}BuLi in Et_2O/toluene at −78 °C, followed by the addition of the appropriate dichloroheteroatom reagent, produced the desired DA products (**Si-DA**, **Ge-DA**, **P-DA**) in quantitative conversion, leading to good isolated yields in all cases.

SCHEME 3

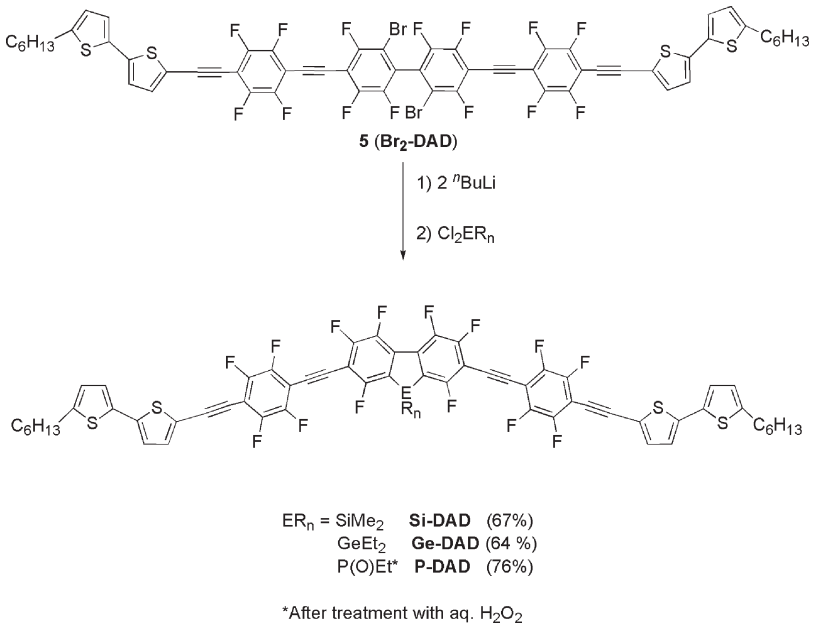

Although the use of S_NAr_F to link the donor and acceptor fragments (as described above) is suitable for small DA precursor molecules like **2**, it is not sufficiently selective for longer DA oligomer or polymer syntheses. To solve this problem the synthetic pathway illustrated in Scheme 2, featuring 1-iodo-4-bromo-tetrafluorobenzene as a linker, was developed. This unsymmetrical linker was made in about 90% conversion (as determined by ^{19}F NMR) from 1,4-dibromotetrafluorobenzene. The 1-iodo-4-bromotetrafluorobenzene was selectively coupled with 2-ethynyl-2′-hexyl-5,5′-bithiophene at the iodo position via a Pd-catalyzed Sonagashira coupling reaction at 45−50 °C (higher temperatures resulted in competitive coupling at the bromo position) to form **3** in 75% isolated yield. In order to successfully couple **3** with 2,2′-dibromo-4-ethynyl-3,3′,4′,5,5′,6,6′-heptafluorobiphenyl (the acceptor monoalkyne fragment), the bromine of **3** must be exchanged for iodine. This was easily accomplished by lithium−halogen exchange of **3** with ^{n}BuLi at −78 °C followed by addition of I_2 in toluene, to produce **4** in 98% isolated yield. Coupling of **4** with the acceptor monoalkyne allowed for quantitative conversion to **2** (as determined by ^{19}F NMR spectroscopy; 56% isolated yield). The synthetic pathway outlined in Scheme 2 is more amenable to the production of DA-containing oligomers and polymers (as compared to that in Scheme 1).

To explore the effect of molecular length and symmetry on the properties of these DA systems, a series of donor−acceptor−donor (DAD) compounds (**Si-DAD**, **Ge-DAD**, **P-DAD**) were also synthesized (Scheme 3). The synthesis of DAD precursor **5** (**Br_2-DAD**) followed a procedure similar to that for the **E-DA** precursor **2**, except that the "acceptor" diyne, 2,2′-dibromo-4,4′-diethynyl-3,3′,5,5′,6,6′-hexafluorobiphenyl, was used in place of the monoyne and two equiv of **4** were required in the final coupling step. Pure **5** was isolated via column chromatography in 90% yield. **E-DAD** compounds **Si-DAD**, **Ge-DAD**, and **P-DAD** were formed by the lithiation of **5** and ^{n}BuLi in Et_2O/toluene at −78 °C, followed by addition of the appropriate dichloroheteroatom reagent (Scheme 3).

To investigate the effect of an alternate positioning of donor and acceptor fragments within the molecule, a germanium-based acceptor−donor−acceptor (ADA) molecule (**Ge-ADA**) was synthesized as described in Scheme 4. The starting compound **6** was obtained in nearly quantitative yield by lithiation at the 5,5‴ positions of 3,3‴-dihexyl-2,2′,2″,2‴,5′,5″-quaterthiophene[31] with ^{n}BuLi, followed by addition of I_2. Coupling of **6** with an excess of ethynyltrimethylsilane via a Pd-catalyzed Sonagashira coupling, followed by trimethylsilyl deprotection with K_2CO_3 in a mixture of MeOH/THF/H_2O, produced the synthetic intermediate 2,2‴-diethynyl-4,4‴-dihexyl-5,2′,2″,5‴,5′,5″-quaterthiophene which must be quickly used and handled in nonpolar solvents to avoid decomposition.

The 1-iodo-4-bromo-tetrafluorobenzene linker was coupled with the "donor" diyne via a Pd-catalyzed Sonagashira coupling reaction to form **7** in high conversion (>85% by ^{19}F NMR spectroscopy, 42% isolated yield). Lithium−halogen exchange of **7** with ^{n}BuLi at −78 °C, followed by the addition of a solution of I_2 in THF, resulted in quantitative conversion to **8** (97% isolated yield). Coupling of **8** with 2 equiv of the "acceptor" monoalkyne allowed high conversion to the ADA precursor **9** (**Br_2-ADA**, 95% by ^{19}F NMR spectroscopy, 67% isolated yield). The final **Ge-ADA** compound was formed by the lithiation of **9** with ^{n}BuLi in THF/toluene at −78 °C, followed by addition of dichlorodiethylgermane.

Computational Studies. To further investigate the electronic structures of the DA compounds, minimized structures of **Si-DA′** and **2T-C_6F_4** (Figure 1) were calculated using the Gaussian 98 suite of programs. Minimized structures and energies were determined using the B3LYP/6-31G(d) level of theory. For ease of calculation, the hexyl groups on the bithiophene fragment

(31) Kanato, H.; Takimiya, K.; Otsubo, T.; Aso, Y.; Nakamura, T.; Araki, Y.; Ito, O. *J. Org. Chem.* **2004**, *69*, 7183.

SCHEME 4

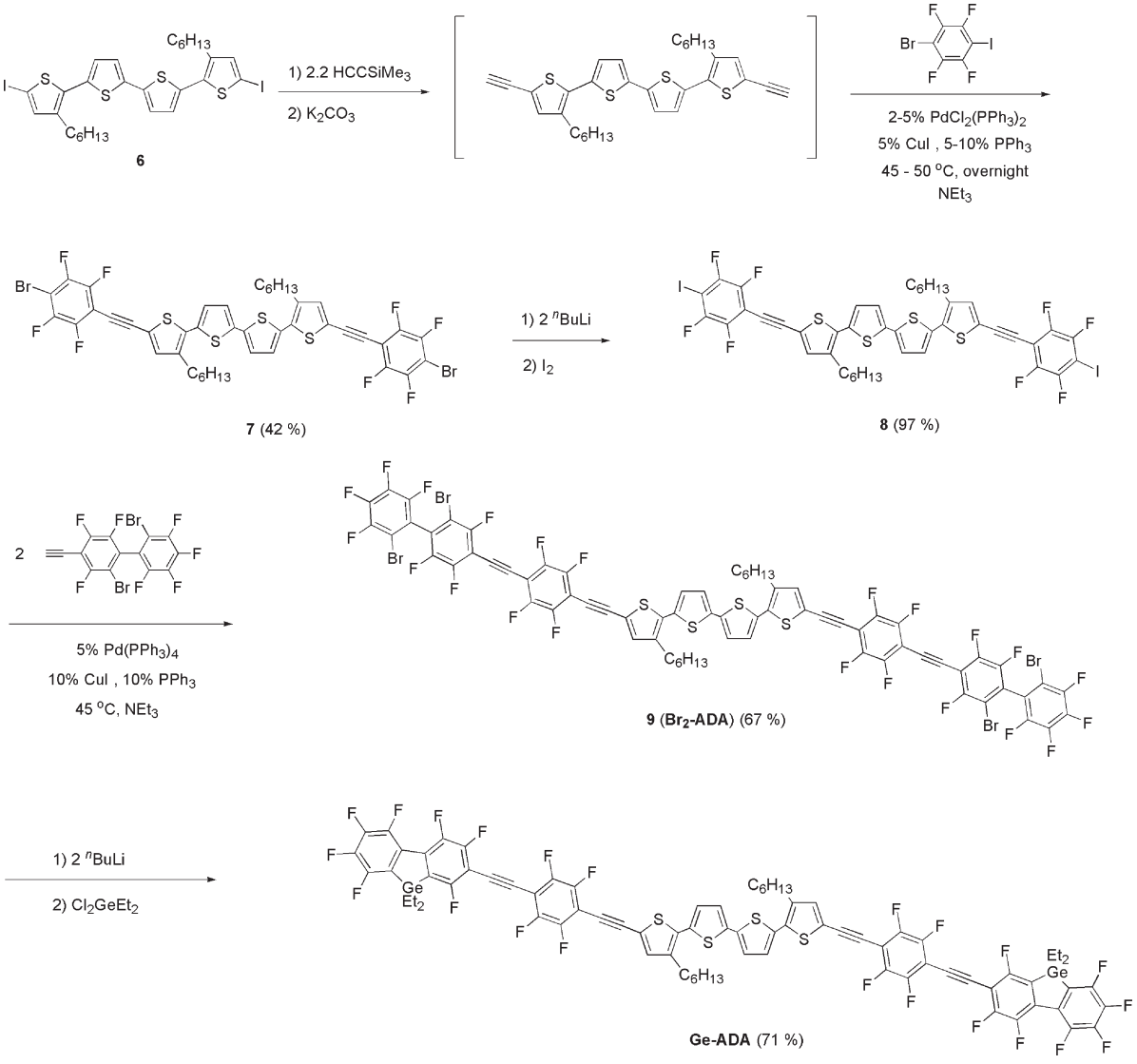

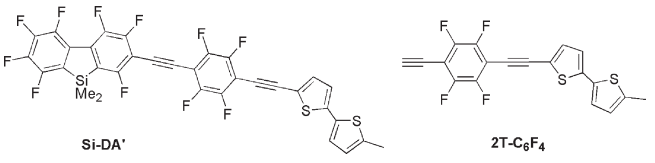

FIGURE 1. Compounds used in computational studies.

were modeled as methyl groups. Of particular interest is the distribution of the HOMO and LUMO orbital wave functions. One extreme possibility would involve a somewhat even distribution of the orbital densities across the entire molecule, thus resembling a more purely p- or n-type system.[14a,32] Alternatively, the HOMO and LUMO molecular orbitals could be concentrated on the electron-rich and electron-poor regions, respectively, producing characteristics more typical of push−pull systems.[33]

Results from the energy minimization of **Si-DA′** (Figure 2a) and **2T-C$_6$F$_4$** (Figure 3a) predict a highly planar overall structure for the ground state, which should favor electronic communication across the entire molecule. As illustrated in Figure 2b,c the HOMO and LUMO orbitals of **Si-DA′** have significant contributions from the central 1,4-diethynyl-tetrafluorophenyl moiety. However, the HOMO orbital density is shifted substantially toward the bithiophene substituent with very little contribution from the heptafluorosilafluorene fragment. The LUMO orbital density is delocalized across the entire molecule; however, the largest contributions come from the fluorinated fragments, with only minimal contribution from the terminal thiophene ring. Similar results were obtained with **2T-C$_6$F$_4$** (Figure 3).

This predicted asymmetry in the HOMO and LUMO orbital distributions indicate that these planar molecules exhibit a break in conjugation. This orbital character could

(32) Radke, K. R.; Ogawa, K.; Rasmussen, S. *Org. Lett.* **2005**, *7*, 5253.

(33) (a) Huang, J.; Fu, H.; Wu, Y.; Chen, S.; Shen, F.; Zhao, X.; Liu, Y.; Yao, J. *J. Phys. Chem. C.* **2008**, *112*, 2689. (b) Rajkumar, G. A.; Sandanayaka, A. S. D.; Ikeshita, K.-I.; Itou, M.; Araki, Y.; Furusho, Y.; Kihara, N.; Ito, O.; Takata, T. *J. Phys. Chem. A.* **2005**, *109*, 2428. (c) Takahashi, S.; Nozaki, K.; Kozaki, M.; Suzuki, S.; Keyaki, K.; Ichimura, A.; Matsushita, T.; Okada, K. *J. Phys. Chem. A.* **2008**, *112*, 2533. (d) Peng, Q.; Park, K.; Lin, T.; Durstock, M.; Dai, L. *J. Phys. Chem. B.* **2008**, *112*, 2801.

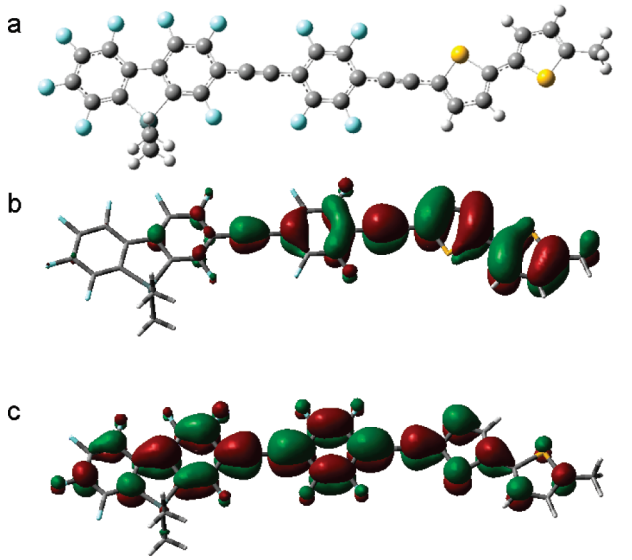

FIGURE 2. Gas-phase computational results for **Si-DA′**. (a) Optimized ground-state geometry emphasizing the planarity of the calculated structure. (b) Calculated HOMO wave function with the majority of the orbital density localized on the bithiophene portion of the molecule. (c) Calculated LUMO wave function.

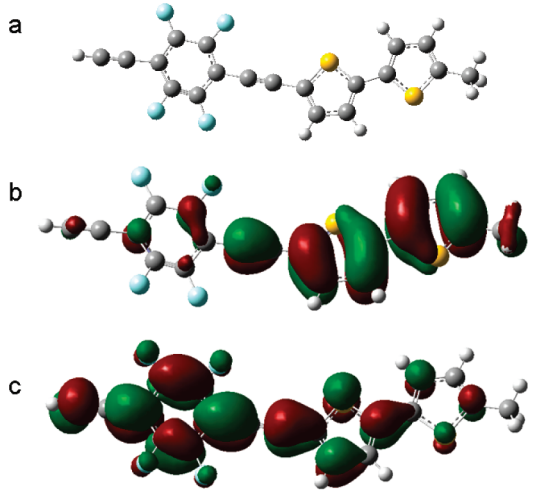

FIGURE 3. Gas-phase computational results for **2T-C$_6$F$_4$**. (a) Optimized ground-state geometry emphasizing the planarity of the calculated structure. (b) Calculated HOMO wave function with the majority of the orbital density localized on the bithiophene. (c) Calculated LUMO wave function.

produce significant charge reorganization in a photoexcited state, perhaps even the generation of a charge-separated excited state.[33] Experimental evidence for this would be interesting, as charge separation is required for the generation of unbound charge carriers in PV applications.[33d] Additionally, significant differences in HOMO and LUMO orbital wave functions can give rise to a large change in dipole between the ground state and the excited state, which has been shown to produce materials with interesting nonlinear optical properties.[7] Finally, the noncontinuous nature of the HOMO and LUMO orbital distributions suggests that oligomers and polymers of these D−A units would not exhibit extended conjugation lengths and a corresponding, reduced band gap, as has been observed for many DA polymers.[32]

TABLE 1. Selected Electrochemical Data for DA Compounds

	LUMO[a] (eV)	HOMO[a] (eV)	E_g^{EC} (eV)	E_g^{opt} (eV)
Si-A	−3.2[b]	−6.5[b]		3.3
Ge-A	−3.2[b]	−6.5[b]		3.3
P-A	−3.4[b]	−6.6[b]		3.2
4	−2.6	−5.7	3.1	3.1
2 (Br$_2$-DA)	−2.8	−5.7	2.9	2.7
Si-DA	−3.3	−5.7	2.4	2.7
Ge-DA	−3.3	−5.7	2.4	2.7
P-DA	−3.5	−5.7	2.2	2.6
5 (Br$_2$-DAD)		−5.7		2.7
Si-DAD	−3.4	−5.7	2.4	2.6
Ge-DAD	−3.4	−5.7	2.4	2.7
P-DAD	−3.6	−5.8	2.2	2.6
Ge-ADA	−3.3	−5.5	2.2	2.4

[a]Referenced to Fc/Fc$^+$ (HOMO energy level −4.8 eV below vacuum).[34] [b]Measured in MeCN with 0.1 M Bu_4NPF_6; calculated HOMO energy from HOMO energy = LUMO energy − E_g^{opt}.

Electrochemical Studies on Donor−Acceptor Compounds. The solution-state redox behavior of all compounds was investigated via differential pulse voltammetry (reduction and oxidation potentials) and the relevant results are summarized in Table 1. All measurements were performed in a CH_3CN/toluene electrolyte solution (0.1 M solution of tetrabutylammonium hexafluorophosphate in CH_3CN/toluene) with a Ag wire reference electrode. HOMO and LUMO energy levels were calculated with respect to the appropriate ferrocene-ferrocenium (Fc/Fc$^+$) oxidation or reduction (Fc HOMO energy of −4.8 eV relative to vacuum).[34] Also included in Table 1 are results from the acceptor-only compounds (**E-A**) (2,7-bis(pentafluorophenylethynyl)-9,9-dimethyl-hexafluorosilafluorene (**Si-A**), 2,7-bis(pentafluorophenylethynyl)-9,9-diethyl-hexafluorogermafluorene (**Ge-A**), and 2,7-bis(pentafluorophenylethynyl)-9-ethyl-hexafluorophosphafluorene oxide (**P-A**)).[21]

The measured LUMO energy levels for the DA compounds, −3.3 to −3.6 eV, are in a range established for useful n-type conducting materials.[4,16,35−37] These LUMO energy levels are significantly lower than those of related nonfluorinated heterofluorenes (−2.1 to −2.6 eV)[35−37] and only slightly lower than those observed for the related 2,7-bis(pentafluorophenylethynyl)-hexafluoroheterofluorenes.[21] This relatively small decrease in LUMO energy (e.g., **Si-A** vs **Si-DAD**), despite a significant increase in conjugation length with the addition of the donor fragment, suggests that the thiophene moieties contribute only slightly to the LUMO energy. Additionally, the similarity of the LUMO energy levels of **Ge-DA** and **Ge-ADA** compounds suggests no greater delocalization of the LUMO orbital in **Ge-ADA** despite an effective increase of the conjugation length of the molecule.

The HOMO energy levels of the DA compounds, −5.5 to −5.8 eV, represent a significant increase over the calculated HOMO energy of the acceptor-only molecules (**Si-A**, **Ge-A**, and **P-A**) of around −6.5 eV and correlate quite well with reported bithiophene and quaterthiophene HOMO energy

(34) Koepp, H. M.; Wendt, H.; Strehlow, H. *Z. Elektrochem.* **1960**, *64*, 483.
(35) Huang, T.-H.; Whang, W.-T.; Shen, J. Y.; Wen, Y.-S.; Lin, J. T.; Ke, T.-H.; Chen, L.-Y.; Wu, C.-C. *Adv. Funct. Mater.* **2006**, *16*, 1449–1456.
(36) Mo, Y.; Tian, R.; Shi, W.; Cao, Y. *Chem. Commun.* **2005**, 4925.
(37) Lee, B. L.; Yamamoto, T. *Macromolecules* **1999**, *32*, 1375–.

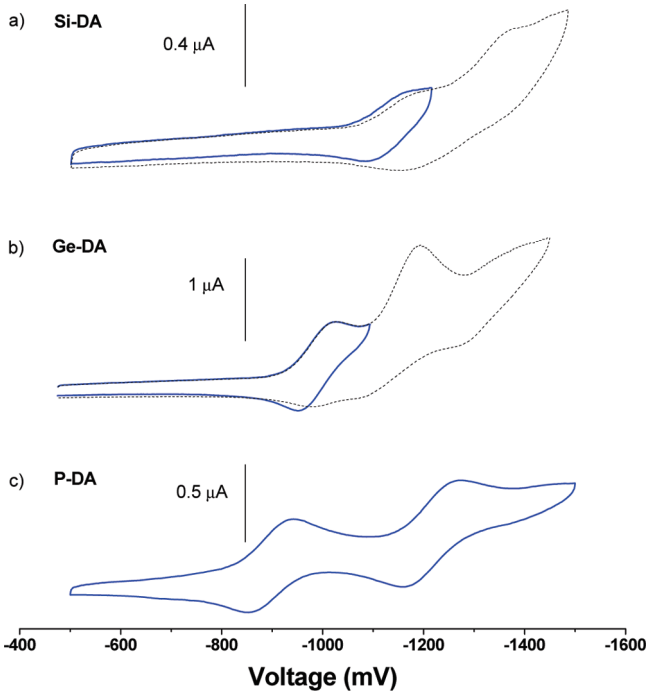

FIGURE 4. Cyclic voltammetry curves for the **E-DA** series. The dotted lines represent subsequent irreversible reductions.

levels (−5.65 and −5.45 eV, respectively).[38] Evaluation of the redox behavior of **4** reveals the similarity of the HOMO energy levels for compounds **4**, **2** (**Br_2-DA**), **E-DA**, and **E-DAD**, which corroborates the theory that the donor fragment is chiefly responsible for the oxidation behavior of these compounds. An increase in the length of the donor fragment, from bithiophene to quarterthiophene, results in a notable destabilization of the HOMO energy (of 0.2 eV), further supporting the participation of this fragment in the HOMO orbital distribution. Finally, the similarity of the HOMO energy levels of the **E-DA** and **E-DAD** compounds suggests there is no electronic communication between the two bithiophene units in the latter, disubstituted **E-DAD** compounds.

The reversibility of the reduction behavior for compounds **Si-DA**, **Ge-DA**, and **P-DA** was investigated via cyclic voltammetry (CV) (Figure 4). As has been observed in previous studies, the reversibility of the solution-state reduction of the fluorinated heterofluorenes varies with changes in the heteroatom.[20,21] **P-DA** exhibits two reversible reduction peaks, and this behavior is consistent with previously studied fluorinated phosphafluorene oxide molecules.[21,22] Both **Si-DA** and **Ge-DA** exhibit multiple reduction events, although only the first of these can be considered either quasi-reversible (**Si-DA**) or reversible (**Ge-DA**). This reversibility behavior is consistent with reduction events dominated by the heterofluorene ring system.[20,21] Oxidation behavior, when observed, is always irreversible. Poor solubility of the **E-DAD** and **Ge-ADA** compounds in the electrolyte solution precluded the collection of meaningful CV data; thus it is not possible to make conclusions about the reversibility of redox events for these compounds.

Many donor−acceptor systems exhibit significant orbital delocalization across both donor and acceptor fragments, resulting in HOMO and LUMO energy levels that are greatly influenced by both fragments.[8a,20,39] However, there are also numerous examples in which the LUMO energy level is dependent solely on the electron-withdrawing fragment and the HOMO energy level is governed predominantly by the electron-donating fragment.[38,40,41] The compounds in this study demonstrate redox chemistry that is consistent with the second type of DA system, as both the reduction and oxidation potentials, as well as the reversibility behavior, seem to correlate with the individual donor or acceptor fragments. These types of donor−acceptor systems have attracted considerable interest with respect to their potential involvement in applications that require charge separation for optimal device performance (e.g., PV).[33d]

Spectroscopic Characterization of Donor−Acceptor Compounds. All UV−vis spectra were recorded in THF and toluene solutions, and relevant data are summarized in Table 2. The corresponding optical HOMO−LUMO energy gaps (E_g^{opt}) were calculated from the absorption onset wavelength, which was taken to be the intersection of the leading edge tangent with the *x*-axis in a standard absorption vs wavelength plot. Also included in Table 2, for comparison, are results from the pure acceptor compounds (**E-A**) (2,7-bis(pentafluorophenylethynyl)-9,9-dimethyl-hexafluorosilafluorene (**Si-A**), 2,7-bis(pentafluorophenylethynyl)-9,9-diethyl-hexafluorogermafluorene (**Ge-A**), and 2,7-bis(pentafluorophenylethynyl)-9-ethyl-hexafluorophosphafluorene oxide (**P-A**)), and the precursor compounds **2** (**Br_2-DA**), **5** (**Br_2-DAD**), **9** (**Br_2-ADA**), and 4,4′-bis(ethynylpentafluorophenyl)-2,2′-dibromo-hexafluorobiphenyl (**Br_2-A**).

The UV−vis spectra of all DA compounds exhibit at least two intense peaks, as illustrated in Figure 5a for the germafluorene-containing series **Ge-DA**, **Ge-DAD**, **Ge-ADA**. (Note: the second peak for the **Ge-DAD** compound appears as a high energy shoulder on the lower energy peak.) Molar absorptivities, ε, were measured for a representative subset of compounds and are reported in Table 2. The strong intensities of the lowest energy transitions (ε = 37 000−100 000 M^{-1} cm^{-1}), coupled with the observation that ε values for **Br_2-DAD** (**5**) and **Ge-DAD** are twice those of **Br_2-DA** (**2**) and **Si-DA** (Table 2), respectively, allow the assignment of the lowest energy peak to a $\pi \rightarrow \pi^*$ transition associated with the thiophene fragment. This conclusion is further supported, in Figure 5b, by the similarity in shape between the absorption spectra of 2′-ethynyl-5,5′-bithiophene (in toluene) and compound **4**, (5-(1-ethynyl-4-iodotetrafluorophenyl)-5′-hexyl-2,2′-bithiophene in THF), the low-energy peaks of **2** (**Br_2-DA**) and **5** (**Br_2-DAD**), and the molar absorptivity value for **4** (ε = 31 000, consistent with a $\pi \rightarrow \pi^*$ transition).

(38) Hancock, J. M.; Gifford, A. P.; Champion, R. D.; Jenekhe, S. A. *Macromolecules* **2008**, *41*, 3588.

(39) (a) Aviram, A.; Ratner, M. *Chem. Phys. Lett.* **1974**, *29*, 277. (b) Sonar, P.; Singh, S. P.; Sudhakar, S.; Dodabalapur, A.; Sellinger, A. *Chem. Mater.* **2008**, *20*, 3184. (c) Sung, H.-H.; Lin, H.-C. *Macromolecules* **2004**, *37*, 7945.

(40) (a) Bauer, P.; Wietasch, H.; Lindner, S.; Thelakkat, M. *Chem. Mater.* **2007**, *19*, 88. (b) Wan, J.-H.; Feng, J.-C.; Wen, G.-A.; Wei, W.; Fan, Q.-L.; Wang, C.-M.; Wang, H.-Y.; Zhu, R.; Yuan, X.-D.; Huang, C.-H.; Huang, W. *J. Org. Chem.* **2006**, *71*, 2565. (c) Tonzola, C. J.; Alam, M. M.; Jenekhe, S. A. *Macromolecules* **2005**, *38*, 9539.

(41) Strehmel, B.; Sarker, A. M.; Malpert, J. H.; Strehmel, V.; Seifert, H.; Neckers, D. C. *J. Am. Chem. Soc.* **1999**, *121*, 1226.

TABLE 2. Steady-State Solution Optical Characterization Data for DA Compounds

	THF				toluene			
	λ_{abs} (nm) (ε, M^{-1} cm^{-1})	E_g^{opt} (eV)[a]	λ_{ems} (nm)[b]	Φ_{PL}[c]	λ_{abs} (nm)	E_g^{opt} (eV)[a]	λ_{ems} (nm)[b]	Φ_{PL}[c]
Br_2-A	306	3.8						
Si-A	349	3.3	378	~1				
Ge-A	347 (61 000)	3.3	376	~1	349	3.3	378	~1
P-A	355	3.2	391	~1				
2 (Br_2-DA)	405 (37 000)	2.7						
Si-DA	408 (50 000)	2.7	544	0.12	409	2.7	481	0.30
Ge-DA	406	2.7	538	0.13	408	2.7	482	0.30
P-DA	412	2.6	579	0.03	409	2.6	502	0.28
5 (Br_2-DAD)	406 (76 100)	2.7	556					
Si-DAD	418	2.6	574	0.04	421	2.6	488	0.33
Ge-DAD	413 (100 000)	2.7	558	0.08	414	2.7	485	0.33
P-DAD	417	2.6	532	0.02	418	2.6	512	0.38
9 (Br_2-ADA)	444	2.4						
Ge-ADA	440	2.4	592	0.07	447	2.4	550	0.28

[a]HOMO−LUMO energy gaps (E_g^{opt}) were calculated from the absorption onset wavelength, determined by the intersection of the leading edge tangent with the *x*-axis. [b]Emission energies were measured with 350 nm excitation wavelength light. [c]Photoluminescence quantum yields calculated with respect to 9,10-diphenylanthracene in THF (Φ_{PL} = 0.9) and are corrected for the solvent refractive index when using toluene.

The higher energy peaks (λ^b_{max} ~310 nm) are associated with a $\pi \rightarrow \pi^*$ transition localized on the electron-deficient portion of the molecules. This assignment is supported by the strong intensities of these peaks (ε = 28 000−70 000 M^{-1} cm^{-1}) and by the red shift observed in the λ^b_{max} values upon closure of the heterofluorene ring (cf. **Br_2-DAD**, λ^b_{max} = 322 nm and **Ge-DAD**, λ^b_{max} = 362 nm). This red shift in λ^b_{max} values for the DA compounds is similar to the red shift observed upon closure of the heterofluorene ring in the pure acceptor compounds (cf. **Br_2-A**, λ_{max} = 306 nm and **Ge-A**, λ_{max} = 347 nm, Table 2). (For **Br_2-DAD** and **Ge-DAD**, λ^b_{max} values appear to be slightly red-shifted with respect to the corresponding values for **Br_2-A** and **Ge-A**, as a result of overlap with the bithiophene absorption).

The observed E_g^{opt} values for the donor−acceptor compounds in the study are lower than those observed for the pure acceptor compounds by 0.5−0.9 eV. This decrease in E_g^{opt} is expected, since addition of the donor fragment should increase the conjugation length of the molecule. Interestingly, there is very little difference in the absorption behavior of the **E-DA** and **E-DAD** series of compounds (Table 2, Figure 6), which suggests that the HOMO and LUMO orbitals are not fully delocalized over the entire molecule. These conclusions are supported by the similarity in E_g^{opt} values for the **Br_2-DAD** and **E-DAD** compounds (Table 2), as the lack of a significant decrease in E_g^{opt} upon closure of the heterofluorene ring implies a break in conjugation between the two bithiophene fragments, which is consistent with the electrochemical behavior described previously.

In general, DA compounds may exhibit varying degrees of orbital mixing between the donor and acceptor fragments, as discussed in the pioneering work of Avrim and Ratner on molecular rectifiers.[39a] If the HOMO and LUMO orbitals are delocalized across significant portions of the molecule, the corresponding energy levels are expected to be significantly influenced by both electron-rich and electron-poor fragments.[39] For these molecules, extension of the π-system via linking of DA units or by extension of the donor and/or acceptor fragments will generally result in an increase in conjugation length and a decrease in E_g^{opt}.[39] Different properties result from DA systems in which the HOMO and LUMO orbital densities are primarily localized on the electron-rich and electron-poor fragments, respectively.[33,40] In this situation, an increase in conjugation length is achieved through modification of the donor and acceptor fragments but not by oligomerization/polymerization of the DA units.

On the basis of the spectroscopic and electrochemical data, it appears that the DA compounds in this study are better described by the latter electronic structure, with HOMO and LUMO orbital densities that are substantially localized on the thiophene- and heterofluorene-containing portions, respectively. This situation is generally observed for DA systems that possess a definitive conjugation break between donor and acceptor moieties, resulting from a saturated organic linker or from a geometric constraint which forces the donor and acceptor π-systems into a mutually perpendicular alignment.[33a−c] However, as shown by Huang and co-workers with a thiophene-oxadiazole system[40b] and by Neckers and co-workers with partially fluorinated oligophenylenevinylenes,[41] there is some precedence for "orbitally segregated" electronic structures in planar π-systems.

Compounds with this orbital distribution often exhibit spectroscopic evidence for some degree of charge separation in the ground and/or excited states.[33,40,41] This charge separation can result in complete transfer of an electron from the donor to the acceptor, i.e., DA $\rightarrow$ D^+A^-, or may involve only a partial redistribution of charge ($D^{\delta+}A^{\delta-}$, where $\delta < 1$). Spectroscopic evidence for the formation of a highly polarized, charge-separated state may appear in the absorption behavior (including solvent polarity dependences of λ_{max} and E_g^{opt} values and/or the emergence of a lower energy charge transfer band) or in the emission behavior (including a large Stokes shift between $\lambda_{max,abs}$ and $\lambda_{max,ems}$ values and a dependence of $\lambda_{max,ems}$ and Φ_{PL} values on solvent polarity).[42] Examination of the absorption behavior of the DA compounds in toluene (dielectric constant ε = 2.38) and THF (ε = 7.52) (Table 2 and Figure 7) reveal a lack of solvatochromism in $\lambda_{max,abs}$ and E_g^{opt} values and no evidence for a direct transition from the ground state to a charge-separated excited state.[43]

(42) Lakowicz, J. R. *Principles of Fluorescence Spectroscopy*, 2nd ed.; Kluwer Academic/Plenum Publishers: New York, 1999.

(43) Neuteboom, E. E.; Meskers, S. C. J.; Beckers, E. H. A.; Chopin, S.; Janssen, R. A. J. *J. Phys. Chem. A* **2006**, *110*, 12363.

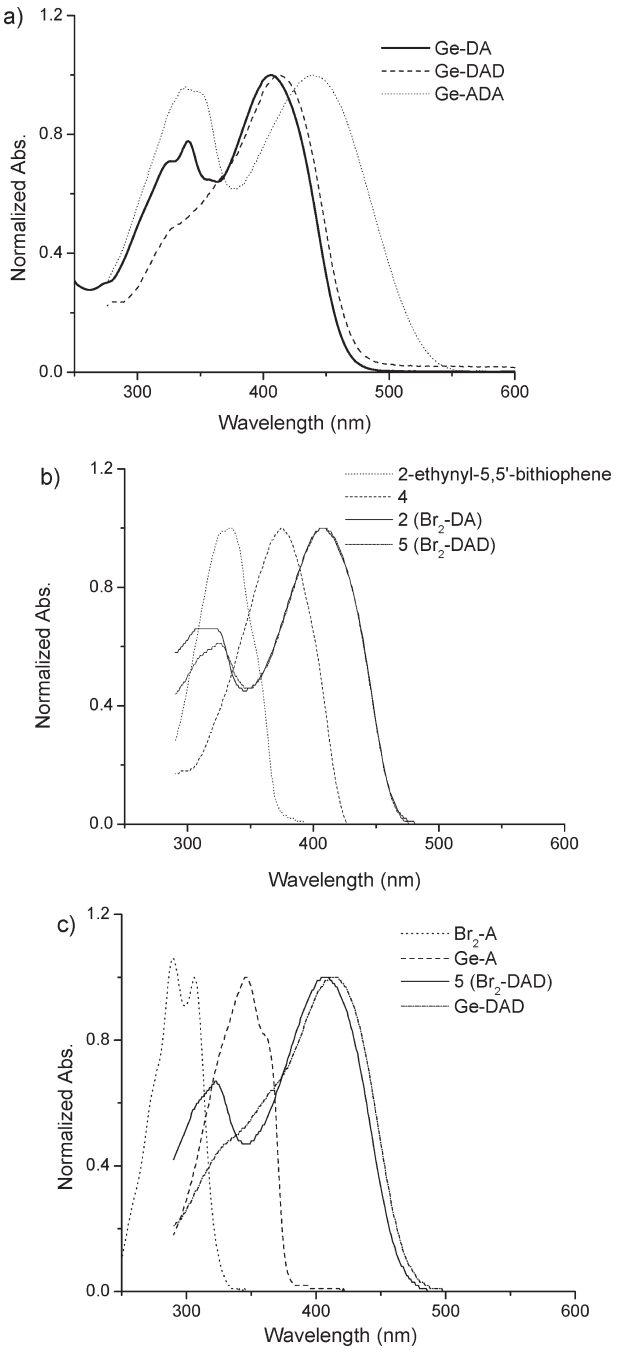

FIGURE 5. Absorption spectra for DA compounds in THF. (a) Changes in absorption for the Ge-series. (b) Changes in absorption spectra with extension of the bithiophene fragment. (c) Comparison of the absorption spectra of acceptor-only and DA compounds.

Photoluminescence spectra were recorded with an optical density of <0.1 in THF and toluene, and relevant data are summarized in Table 2. The emission λ_{max} values for the DA compounds in THF ranged from 530−590 nm and varied with heteroatom, donor length, and acceptor length. These emission wavelengths represent a Stokes shift of about 140−150 nm, which is significantly greater than those typically

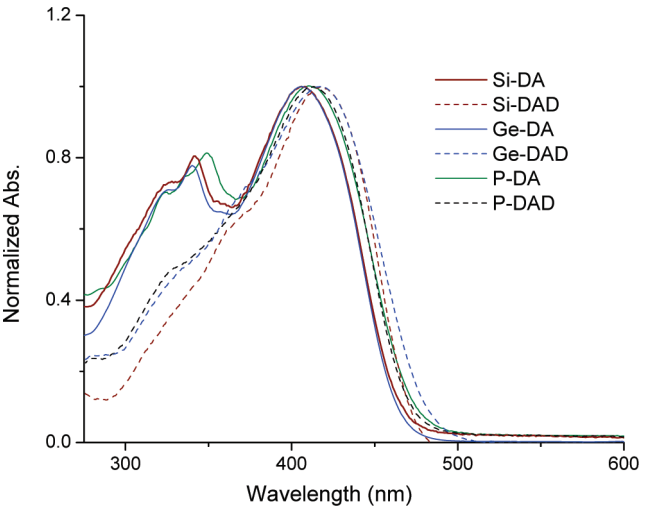

FIGURE 6. UV−vis spectra of the **E-DA** and **E-DAD** series in THF, illustrating the similarity in E_g^{opt} values.

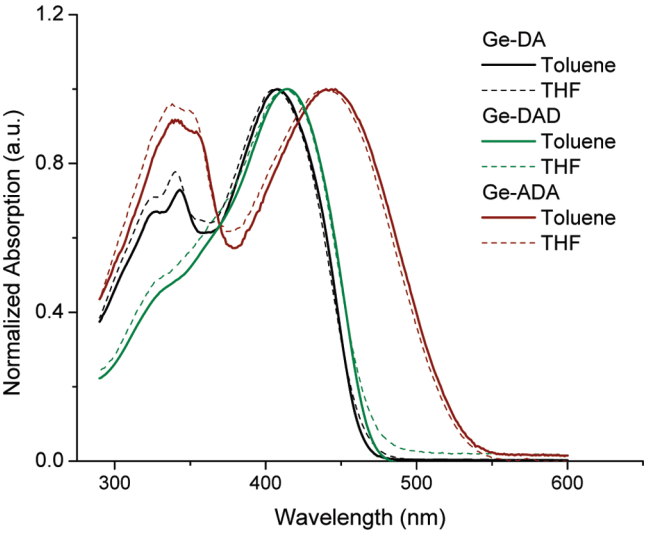

FIGURE 7. UV−vis spectra of the Ge-series of compounds in THF and toluene, illustrating the lack of solvatochromism in the absorption behavior.

observed for 2,7-bis(ethynylpentafluorophenyl)-hexafluoroheterofluorenes (~20 nm)[20,21] and for oligothiophenes (~70 nm).[44] Additionally, the photoluminescence quantum yields (Φ_{PL}) for the DA compounds in THF are 1−2 orders of magnitude lower than those observed for the acceptor-only compounds (**E-A**, Table 2). This dramatic increase in Stokes shifts and the decrease in Φ_{PL} values suggest the possibility of an intramolecular charge separation accompanied by molecular reorganization in the excited state.[42] With toluene as the solvent, the emission maxima of the donor−acceptor compounds are significantly blue-shifted, and the Φ_{PL} values are 3−10 times higher than those observed in THF solvent. This is consistent with less structural reorganization in the excited state in a nonpolar solvent. A more extensive study of the solvent-dependent emission behavior for **Ge-DAD** (Figure 8) reveals a significant red shift in the emission λ_{max} value with increasing solvent polarity (dielectric constant for each solvent is provided in the legend). This strong solvatochromism is also

(44) Sakamoto, Y.; Komatsu, S.; Suzuki, T. *Synth. Met.* **2003**, *133*−*134*, 361.

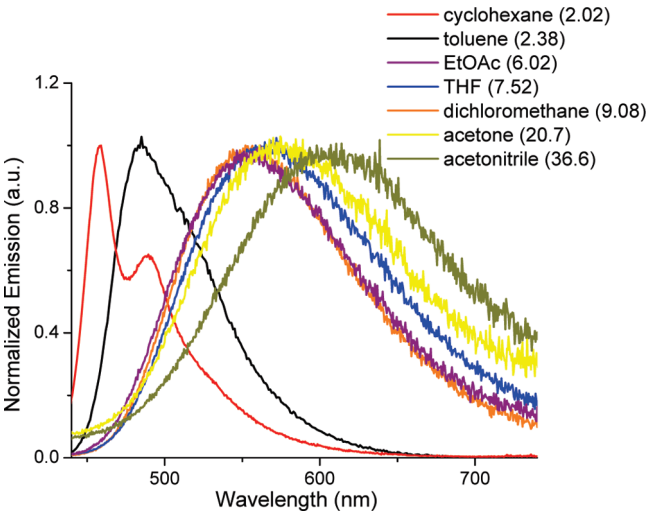

FIGURE 8. Normalized emission spectra for **Ge-DAD** illustrating the red shift in emission λ_{max} value with increasing solvent polarity. The dielectric constant for each solvent is provided in the legend.

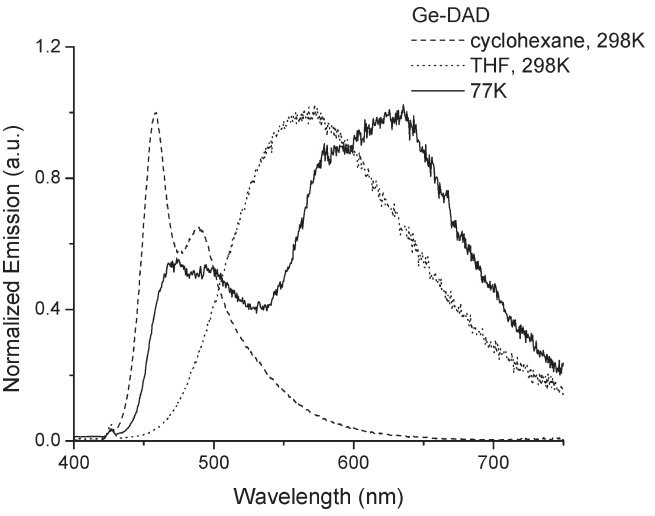

FIGURE 9. Emission spectra for **Ge-DAD** in cylcohexane (298 K), THF (298 K), and 1:4 methanol/ethanol (77 K), λ_{ex} = 380 nm.

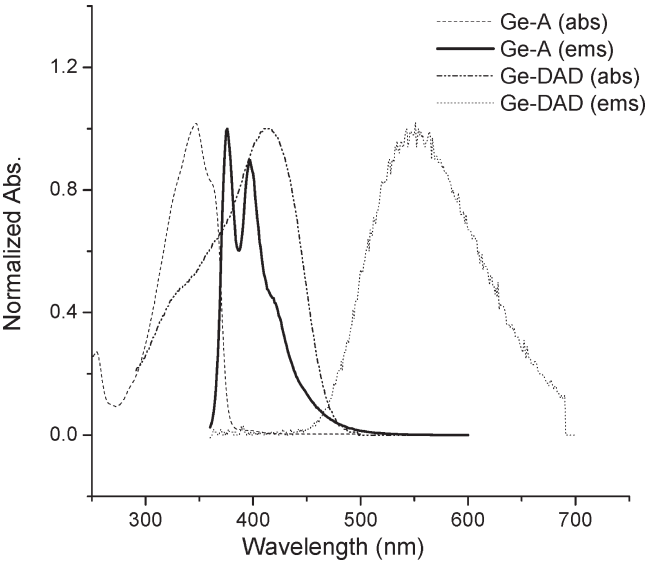

FIGURE 10. Absorption and emission of **Ge-A** and **Ge-DAD** illustrating the overlap in the emission of **Ge-A** and the absorption of **Ge-DAD**.

in agreement with the possible formation of a charge-separated excited state. Additionally, the absence of vibronic structure in solvents expected to better stabilize a polarized intermediate (versus that observed in cyclohexane) is consistent with the idea that emission originates from a charge-separated excited state. The increase in noise observed for the high dielectric constant solvents is due to the decreased emission intensity with these samples, although precise Φ_{PL} values were not calculated (note that Figure 8 reports normalized emission).

Photoinduced intramolecular charge transfer processes, which usually follow Marcus theory, are generally slower at lower temperatures. Thus luminescence spectroscopy at 77K was expected to reveal emission from local excited states only (both singlet and/or triplet states) that are greatly enhanced with respect to that from charge-separated states. The low-temperature (77 K) emission spectrum of **Ge-DAD** (Figure 9) reveals two major peaks at 475 and 635 nm. The high energy emission (at 475 nm) correlates well with the room temperature emission of **Ge-DAD** in cyclohexane (in both vibronic structure and energy) and thus can be assigned to emission from the singlet local excited state. The structured lower energy band (λ = 635 nm and λ = 590 nm) can be assigned to emission from the triplet local excited state.[42] The lack of defined structure and the clear solvatochromism in the room temperature emission behavior of **Ge-DAD** further supports the occurrence of emission from a charge-separated state in all cases except cyclohexane.

Fluorescence lifetime (τ) measurements for **Si-DA**, **Ge-DA**, and **P-DA** in toluene, dichloromethane, and THF reveal decay behavior that is best modeled by a single exponential decay. Fluorescence lifetimes exhibit little dependence on solvent ($\tau \approx 650$ ps for **Si-DA**, **Ge-DA** and $\tau \approx 700-850$ ps for **P-DA**) and confirm that the room temperature emission is from a singlet state and not from a triplet state, as this would result in much longer fluorescence lifetimes. Transient absorption spectroscopy experiments, which could identify the presence of a radical anion and cation, have proven difficult. The required excitation wavelength of 466 nm produces a bleach signal across the absorption region for the bithiophene radical cation (495 nm),[45] and attempts to determine the absorption spectrum for the germafluorene-based radical anion via spectroelectrochemistry experiments have not yet been successful. Attempts to perform TDDFT calculations were unsuccessful as a result of issues with nonconvergence.

While spectroscopic data suggests the formation of a charge-separated state in these DA compounds, other energy transfer mechanisms cannot be completely ruled out. For example, overlap between the emission spectra of the heterofluorene fragments and the absorption spectra for the extended bithiophene fragments (as illustrated for **Ge-DAD** and its component molecules in Figure 10) suggests that a resonance energy transfer from the acceptor to the donor might be possible.[40a,42,46]

(45) Huang, J.; Fu, H.; Wu, Y.; Chen, S.; Shen, F.; Zhao, X.; Liu, Y.; Yao, J. *J. Phys. Chem. C* **2008**, *112*, 2689.
(46) Bauer, P.; Wietasch, H.; Lindner, S.; Thelakkat, M. *Chem. Mater.* **2007**, *19*, 88.

TABLE 3. Selected PV Device Performance Data for Ge- and P-Based Compounds

	V_{oc} (V)[a]	I_{sc} (mA)[b]	J_{sc} (mA/cm^2)[c]	fill factor[d]	η (%)[e]
P3HT-alone	0.040	−1.3	−0.044	0.253	0.0004
Ge-DA/P3HT	0.107	−1.95	−0.065	0.265	0.002
Ge-DAD/P3HT	0.563	−4.9	−0.162	0.333	0.031
Ge-ADA/P3HT	0.298	−7.0	−0.234	0.272	0.019
P-DA/P3HT	0.092	−4.6	−0.154	0.258	0.003
P-DAD/P3HT	0.542	−0.8	−0.025	0.303	0.004
Ge-A/P3HT	0.905	−6.3	−0.211	0.184	0.035
P-A/P3HT	0.743	−1.8	−0.064	0.255	0.012

[a]Open circuit voltages (V_{oc}) were calculated from the x-intercept (zero current value) of the current vs applied potential data. [b]Short circuit currents (I_{sc}) were calculated from the y-intercept (zero voltage value) of the current vs applied potential data. [c]Short circuit current densities (J_{sc}) were calculated by $J_{sc} = I_{sc}$/(pixel area). [d]Fill factor is calculated from the maximum power $IV/I_{sc}V_{oc}$. [e]Efficiency (η) is calculated from $\eta = V_{oc}$ J_{sc} · fill factor/intensity of incoming light.

Preliminary Device Studies. Previous work has demonstrated that photovoltaic (PV) devices fabricated with 2,7-bis(pentafluorophenylethynyl)-hexafluoroheterofluorene/poly-3-hexylthiophene (P3HT) blends have higher overall efficiencies than devices made with P3HT alone.[21] Additionally, the tendency for 2,7-substituted hexafluoroheterofluorenes to pack cofacially in the solid state[20,21] makes these DA compounds excellent candidates for use as charge-transporting materials in solar cells. Although the DA molecule described here should be able to internally separate charge, the length scale is much smaller than an exciton diffusion length, so here we describe devices that use the DA to separate charge within a matrix of P3HT hole transporter.

Preliminary device studies included evaluation of germafluorene (**Ge-DA**, **Ge-DAD**, **Ge-ADA**) and phosphafluorene oxide containing compounds (**P-DA**, **P-DAD**) for use as electron transport materials in PV devices. Unoptimized PV cells were made from 1:1 wt % blends of the DA compound and P3HT that were spin-coated onto an ITO surface from chloroform solution (10 mg/mL, ~80 nm thick films), followed by vapor deposition of an aluminum cathode. The devices were tested under an argon atmosphere with an oriel xenon arc lamp with an AM 1.5G solar filter, and the results are summarized in Table 3. Also included in Table 3 are results from similar devices made using 2,7-bis(pentafluorophenylethynyl)-9,9-diethyl-hexafluorogermafluorene (**Ge-A**) and 2,7-bis(pentafluorophenylethynyl)-9-ethyl-hexafluorophosphafluorene oxide (**P-A**).[21] Figure 11 illustrates the current density−applied voltage performance of the germanium-based series, and additional current−voltage data is available in Supporting Information.

As illustrated in Figure 11 and Table 3, the PV devices made with blends of donor−acceptor compounds/P3HT clearly exhibit improved performance over the P3HT-only devices. This can be attributed to a much higher open circuit voltage (V_{oc}) in most of the blend systems, which results in greater charge separation than in the pure P3HT system. Additionally, in most cases, the short circuit current density (J_{sc}) of the blend devices is significantly larger than that of the pure P3HT system, which suggests that incorporation of the DA molecules improves overall charge transport in the devices. The compounds with longer acceptor fragments have higher open circuit voltages, generally resulting in higher overall efficiencies. The

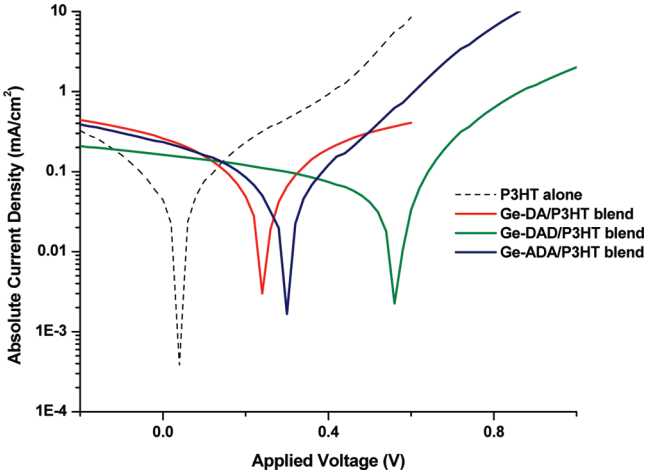

FIGURE 11. Applied voltage-current density performance for P3HT alone and germanium donor−acceptor/P3HT series: **Ge-DA**, **Ge-DAD**, **Ge-ADA**.

germanium-based materials exhibit slightly better performances with respect to their phosphine oxide-based counterparts. In these devices, the presence of the thiophene donor fragment does not improve PV performance. This may be due to the short nature of the donor fragment used (2 or 4 rings) or the small overall size of the DA molecules. The development of longer DA oligomers may lead to improved interactions between P3HT and the donor portion of the DA compounds, resulting in improved intermolecular charge transfer.

The efficiencies of these devices are rather low (0.002−0.031%) compared to those obtained for optimized devices based on P3HT/PCBM (4−5%, PCBM = [6,6]-phenyl-C_{61}-butyric acid methyl ester)[47] and P3HT/perylene diimide (0.5−1%),[48] which may be due to the short length scale of the DA molecules. Further modifications to the structures of such fluorinated, heterofluorene-based compounds to increase donor and acceptor fragment lengths may provide more efficient charge transport. Alternatively the application of these shorter DA molecules might function effectively as blend compatibilizers (both mechanically and electronically) in donor and acceptor homopolymer blend systems.

Concluding Remarks

The oligothiophene-fluorinated heterofluorene systems described here exhibit interesting donor−acceptor (DA) properties. Results from calculations and the optical and electrochemical characterizations suggest that the HOMO and LUMO orbitals do not extend across the full length of the molecules and that the HOMO and LUMO orbital wave functions are mostly localized onto the donor and acceptor fragments, respectively. From these results it can be concluded that further reduction in the HOMO−LUMO energy gap and subsequent improvement in solar radiation spectrum overlap will require extension of the individual donor and/or acceptor moieties. Also, the conjugation lengths of

(47) Backer, S. A.; Sivula, K.; Kavulak, D. F.; Fréchet, J. F. J. *Chem. Mater.* **2007**, *19*, 2927.
(48) Zhan, X.; Tan, Z.; Domercq, B.; An, Z.; Zhang, X.; Barlow, S.; Li, Y.; Zhu, D.; Kippelen, B.; Marder, S. *J. Am. Chem. Soc.* **2007**, *129*, 7246.

these molecules cannot be increased solely through oligomerization or polymerization. While there is no evidence of an intermolecular charge transfer (ICT) in the ground state, the distinct solvatochromism in the photoluminescence suggests a possible charge transfer in the excited state. Clearly the excited-state behavior of the compounds is complex and warrants further investigation.

Preliminary photovoltaic (PV) studies with DA/poly-3-hexylthiophene (P3HT) blends demonstrate improved efficiency over P3HT-only devices, although overall efficiencies are still quite low (< 0.05%). Current research is focused on modification of both the donor and acceptor portions of the molecule to improve solar radiation overlap and on development of improved charge separation and charge transport behavior.

Experimental Section

General. All reactions were performed under an inert atmosphere of nitrogen using standard Schlenk techniques unless otherwise specified. Tetrahydrofuran (THF) was dried over Na and stored under nitrogen. Hexanes, Et_2O, and toluene were dried on a VAC systems solvent purifier column and stored under nitrogen. Dichlorothethylphosphine, hydrogen peroxide (30% in water), butyllithium (1.6 M in hexanes), tetrabutylammonium hexafluorophosphate, dibromotetrafluorobenzene, and dichlorodiethylgermane were used as received. Dichlorodimethylsilane was distilled prior to use. Fluorescence quantum yields (Φ_{PL}) were calculated with respect to freshly sublimed 9,9-diphenylanthracene in THF ($\Phi = 0.90$). Fluorescence lifetime measurements were performed using the time correlated single photon counting (TCSPC) method. The system was equipped with a Triax 320 and a Single Photon Counting Controller and a 440 nm LED NanLED, maximum repetition rate of 1 MHz and a pulse duration < 200 ps. Unless otherwise stated, ^1H, ^{31}P, and ^{19}F NMR spectra were measured in $CDCl_3$ with a 400 MHz spectrometer. All chemical shifts are reported in ppm units. For ^{19}F NMR spectra C_6F_6 was used as internal reference at −163 ppm and ^1H NMR chemical shifts were referenced to the residual peak of the deuterated $CDCl_3$ at 7.26 ppm. Melting point determinations are uncorrected. Cyclic voltammetry potentials were measured versus a Ag wire reference electrode, with Pt disk (PTE) as working electrode and a Pt wire axial electrode, in acetonitrile/toluene (8:2) containing 0.1 mol/L tetrabutylammoniumhexafluorophosphate, with ferrocene as external standard (HOMO = −4.8 eV) and potential sweep rate of 100 mV/s unless otherwise stated.

Lithium triisopropylsilylacetylene was prepared from triisopropylsilylacetylene and ^{n}BuLi in hexanes. 2-Bromo-2′-hexyl-5,5′-bithiophene was prepared by bromination of (5-hexyl-2,2′-bithiophene)[49] with NBS. 2,2′-Dibromooctafluorobiphenyl,[50] 2-bromo-3-hexyl-thiophene,[51] and 3,3‴-dihexyl-2,2′,2″,2‴,5′,5″-tetrathiophene[52,53] were prepared as described in the literature.

The syntheses of intermediate compounds 4-bromo-1-iodotetrafluorobenzene, 2,2′-dibromo-4-ethynyl-3,3′,4′,5,5′,6,6′-heptafluorobiphenyl, and 2,2′-dibromo-4,4′-diethynyl-3,3′,5,5′,6,6′-hexafluorobiphenyl are described below.

4-Bromo-1-iodotetrafluorobenzene. 1,4-Dibromopentafluorobenzene (2.0 g, 6.5 mmol) was dissolved in toluene/Et_2O (100 mL/ 20 mL), and the resulting solution was cooled to −78 °C. To this was added butyllithium (4 mL, 1.6 M in hexanes), and the reaction mixture was stirred for 20 min. Iodine (2.0 g, 7.9 mmol) was dissolved in Et_2O (20 mL), the resulting solution was added to the 1-bromo-4-lithiotetrafluorobenzene, and the resulting reaction mixture was stirred for 10 min at −78 °C. Aqueous $Na_2S_2O_3$ was added, and the reaction mixture was allowed to warm to room temperature with stirring over 1 h. The reaction mixture was washed with water (2 × 50 mL,) and the organic components were dried over $MgSO_4$ and then filtered through Celite. Rotary evaporation of the solution provided white crystals of the following composition: 92% 4-bromo-1-iodotetrafluorobenzene, 5% 1,4-dibromotetrafluorobenzene, and 3%, 4-dibromotetrafluorobenzene, as determined by ^{19}F NMR and GC:MS. 4-Bromo-1-iodotetrafluorobenzene: ^{19}F NMR ($CDCl_3$, 376 MHz, 25 °C) δ −119.67 (1F, m), −132.14 (1F, m); MS 354 (M^+). 1,4-Dibromotetrafluorobenzene: ^{19}F NMR ($CDCl_3$, 376 MHz, 25 °C) δ −132.54 (s); MS 308 (M^+). 1,4-Dibromotetrafluorobenzene: ^{19}F NMR ($CDCl_3$, 376 MHz, 25 °C) δ −119.40 (s); MS 402 (M^+).

2,2′-Dibromo-4,4′-diethynyl-3,3′,5,5′,6,6′-hexafluorobiphenyl. To a solution of 2,2′-dibromooctafluorobiphenyl (0.230 g, 0.5 mmol) in toluene (25 mL) at room temperature was added a solution of lithium triisopropylsilylacetylide (0.210 g, 1.1 mmol) in THF (8 mL). The resulting solution was stirred for 3−5 days. The resulting yellow solution was washed with water (2 × 30 mL). The organic components were dried over $MgSO_4$ and filtered through Celite. The resulting solution was then diluted with wet toluene (600 mL) and distilled THF (45 mL). The solution was sparged with nitrogen for 20 min, and then Bu_4NF (1.1 mL, 1.0 M in THF 1% H_2O) was added. The resulting mixture was stirred for 5 min. The light brown solution was washed with water (2 × 150 mL), and the organic components were dried over $MgSO_4$ and passed through a silica plug. The resulting solution was concentrated via rotary evaporation. *Note: It is critical at this step to not combine concentrated solutions of unprotected diyne with THF or CH_2Cl_2. This will result in decomposition of the compound.* The resulting solution was absorbed onto silica and the diyne was isolated via column chromatography and used without further purification. ^1H NMR ($CDCl_3$, 400 MHz, 25 °C) δ 3.737 (s); ^{19}F NMR ($CDCl_3$, 376 MHz, 25 °C) δ −102.99 (1F, m), −130.68 (1F, m), −137.38 (1F, m); MS 462 (M^+), 383, 302.

2,2′-Dibromo-4-ethynyl-3,3′,4′,5,5′,6,6′-heptafluorobiphenyl. To a solution of 2,2′-dibromooctafluorobiphenyl (0.500 g, 1.1 mmol) in toluene (20 mL) at room temperature was added a solution of lithium triisopropylsilylacetylide (0.244 g, 1.3 mmol) in THF (5 mL), and the resulting solution was stirred for 3−5 days. The resulting yellow solution was washed with water (2 × 30 mL) and the organic components were dried over $MgSO_4$ and filtered through Celite. The resulting solution was then diluted with wet toluene (800 mL) and distilled THF (40 mL) and was then sparged with nitrogen for 20 min. Under a flow of nitrogen, Bu_4NF (1.1 mL, 1.0 M in THF 1% H_2O) was added, and the resulting solution was stirred for 5 min. The light brown solution was washed with water (2 × 150 mL) and the organic components were dried over $MgSO_4$ and passed through a silica plug. The resulting solution was concentrated via rotary evaporation. *Note: It is critical at this step not to combine concentrated solutions of unprotected alkyne with THF or CH_2Cl_2. This will result in decomposition of the compound.* The resulting solution was absorbed onto silica and the monoyne was isolated via column chromatography and used without further purification. ^1H NMR ($CDCl_3$, 400 MHz, 25 °C) δ 3.737 (s); ^{19}F NMR ($CDCl_3$, 376 MHz, 25 °C) δ −101.86 (1F, m), −128.47 (1F, m), −130.68 (1F, m), −135.34 (1F, m), −137.30 (1F, m), −150.90 (1F, m), −155.00 (1F, m). MS: 462 (M^+), 383, 302.

(49) Sotgiu, G.; Zambianchi, M.; Barbarella, G.; Botta, C. *Tetrahedron* **2002**, *58*, 2245.
(50) Cohen, S.; Fenton, D.; Tomlinson, A.; Massey, A. *J. Organomet. Chem.* **1966**, *6*, 301.
(51) Takahashi, M.; Masui, K.; Sekiguchi, H.; Kobayashi, N.; Mori, A.; Funahashi, M.; Tamaoki, N. *J. Am. Chem. Soc.* **2006**, *128*, 10930.
(52) Kanato, H.; Takimiya, K.; Otsubo, T.; Aso, Y.; Nakamura, T.; Araki, Y.; Ito, O. *J. Org. Chem.* **2004**, *69*, 7183.
(53) Radke, K. R.; Ogawa, K.; Rasmussen, S. *Org. Lett.* **2005**, *7*, 5253.

2,2′-Dibromo-4-pentafluorophenylethynyl-heptafluorobiphenyl (1). To a solution of 2,2′-dibromooctafluorobiphenyl (0.500 g, 1.1 mmol) in toluene (20 mL) at room temperature, a solution of lithium triisopropylsilylacetylide (0.244 g, 1.3 mmol) in THF (5 mL) was added, and the resulting solution was stirred for 3−5 days. The resulting yellow solution was washed with water (2 × 30 mL), and the organic components were dried over $MgSO_4$ and filtered through Celite. The resulting solution was then diluted with wet toluene (800 mL) and distilled THF (40 mL) and was then sparged with nitrogen for 20 min. Under a flow of nitrogen, Bu_4NF (1.1 mL, 1.0 M in THF 1% H_2O) was added, and the resulting solution was stirred for 5 min. The light brown solution was washed with water (2 × 150 mL), and the organic components were dried over $MgSO_4$ and passed through a silica plug. The resulting solution was concentrated via rotary evaporation. *Note: It is critical at this step not to combine concentrated solutions of unprotected alkyne with THF or CH_2Cl_2. This will result in decomposition of the compound.* The resulting solution was absorbed onto silica, and the monoyne was isolated via column chromatography. 2,2′-Dibromo-4-ethynyl-3,3′,4′,-5,5′,6,6′-heptafluorobiphenyl and iodopentafluorobenzene (0.7 mL, 2.4 mmol) were combined with NEt_3 (10 mL), and the resulting solution was sparged with nitrogen for 10 min. The degassed solution was added to a Schlenk flask containing $PdCl_2(PPh_3)_2$ (0.05 g, 0.07 mmol), CuI (0.06 g, 0.3 mmol), and PPh_3 (0.06 g, 0.2 mmol), and the entire mixture was heated at 40 °C for 12 h, with vigorous stirring, under a flow of nitrogen. Toluene (20 mL) was added to the solution, and the resulting mixture was washed with aqueous NH_4Cl (2 × 20 mL) and water (2 × 20 mL). The combined organic components were dried with $MgSO_4$, filtered through Celite, and concentrated via rotary evaporation. The monosubstituted product was isolated via column chromatography (hexanes) to give 0.295 g (0.47 mmol, 43%) of **1** as a white powder. ^{19}F NMR ($CDCl_3$, 376 MHz, 25 °C) δ −101.73 (1F, m), −128.35 (1F, m), −129.61 (1F, m), −135.30 (1F, m), −135.41 (2F, m), −136.81 (1F, m), −150.43 (1F, m), −150.68 (1F, m), −154.86 (1F, m), −161.90 (2F, m). Anal. Calcd for $C_{28}Br_2F_{16}$: C, 38.25. Found: C, 38.11. Mp 132−135 °C.

2,2′-Dibromo-4-(1-(5-ethynyl-5′-hexyl-2,2′-bithienyl)-4-ethynyltetrafluorophenyl)-heptafluorobiphenyl (2). Method 1. Trimethylsilylacetylene (0.05 mL, 1.2 mmol) was combined with NEt_3 (30 mL), and the entire solution was sparged with nitrogen for 10 min. The degassed solution was added to a Schlenk flask containing 2-bromo-2′-hexyl-5,5′-bithiophene (0.150 g, 0.47 mmol), $PdCl_2(PPh_3)_2$ (0.030 g, 0.03 mmol), CuI (0.020 g, 0.10 mmol), and PPh_3 (0.020 g, 0.08 mmol), and the entire mixture was heated at 40 °C for 12 h, with vigorous stirring, under a flow of nitrogen. Toluene (20 mL) was added to the solution, and the resulting mixture was washed with aqueous NH_4Cl (2 × 20 mL) and water (2 × 20 mL). The organic components were dried over $MgSO_4$, filtered through Celite, and concentrated via rotary evaporation. The resulting solid was redissolved in hexanes, passed through an alumina plug, and concentrated via rotary evaporation. The resulting 5-ethynyltrimethylsilyl-5′-hexyl-2,2′-bithiophene was dissolved in a mixture of THF/MeOH/H_2O (5 mL/5 mL/2 mL) and stirred with K_2CO_3 (0.050 g, 0.36 mmol) for 3 h. Hexanes (20 mL) were added to the solution, and the mixture was washed with water (2 × 20 mL). The organic components were dried over $MgSO_4$, filtered through Celite, and concentrated via rotary evaporation. The resulting viscous oil was dissolved in hexanes (5 mL), the resulting solution was transferred to a Schlenk flask, and the solvent was then removed under vacuum. The resulting viscous oil was combined with THF (2 mL), to this was added butyllithium (0.14 mL, 1.6 M in hexanes), and the solution was stirred for 20 min at room temperature. In a separate Schlenk flask, 2,2′-dibromo-4-(pentafluorophenylethynyl)-heptafluorobiphenyl (**1**) (0.140 g, 0.22 mmol) was dissolved in toluene/THF (40 mL/10 mL) and cooled to 0 °C. To this solution of **1** was added the alkynyl lithium, and the reaction mixture was allowed to warm to room temperature with stirring over 24 h. The resulting yellow solution was quenched with water (2 × 15 mL), and the organic components were extracted into CH_2Cl_2 (2 × 20 mL). The combined extracts were dried over $MgSO_4$, filtered through Celite, and concentrated via rotary evaporation. The resulting solid was absorbed onto silica gel and purified by column chromatography (hexanes/toluene 100:5) to give 0.120 g (59%, 0.13 mmol) of **2** as a light orange powder.

Method 2. 2,2′-Dibromo-4-ethynyl-3,3′,4′,5,5′,6,6′-heptafluorobiphenyl (0.6 g, 1.3 mmol) and **4** (0.200 g, 0.36 mmol) were dissolved in NEt_3 (30 mL), and the solution was sparged with nitrogen for 10 min. The degassed solution was added to a Schlenk flask containing $Pd(PPh_3)_4$ (0.050 g, 0.04 mmol), CuI (0.040 g, 0.21 mmol), and PPh_3 (0.040 g, 0.15 mmol), and the entire mixture was heated at 40 °C for 12 h, with vigorous stirring, under a flow of nitrogen. Toluene (20 mL) was added to the solution, and the resulting mixture was washed with aqueous NH_4Cl (2 × 20 mL) and water (2 × 20 mL). The organic components were dried over $MgSO_4$, filtered through Celite, and concentrated via rotary evaporation. The resulting solid was absorbed onto silica gel and purified by column chromatography (hexanes/toluene 100:5) to give 0.180 g (56%, 0.2 mmol) of **2** as a light orange powder. ^1H NMR ($CDCl_3$, 400 MHz, 25 °C) δ 0.888 (3H, t), 1.3−1.4 (6H, m), 1.667 (2H, q), 2.806 (2H, t), 6.714 (1H, d), 7.039 (1H, d), 7.063 (1H, d), 7.325 (1H, d); ^{19}F NMR ($CDCl_3$, 376 MHz, 25 °C) δ −101.59 (1F, m), −128.38 (1F, m), −129.50 (1F, m), −135.27 (1F, m), −136.85 (3F, m), −137.56 (2F, m), −150.71 (1F, m), −154.87 (1F, m). Anal. Calcd for $C_{36}H_{17}Br_2F_{11}S_2$: C, 49.00; H, 1.94; S, 7.27. Found: C, 48.81; H, 1.80; S, 7.17. Mp 144−146 °C.

5-(1-Ethynyl-4-bromo-tetrafluorophenyl)-5′-hexyl-2,2′-bithiophene (3). Trimethylsilylacetylene (0.2 mL, 5 mmol) was combined with NEt_3 (30 mL), and the entire solution was sparged with nitrogen for 10 min. The degassed solution was added to a Schlenk flask containing 2-bromo-2′-hexyl-5,5′bithiophene (0.180 g, 0.55 mmol), $PdCl_2(PPh_3)_2$ (0.030 g, 0.03 mmol), CuI (0.020 g, 0.10 mmol), and PPh_3 (0.020 g, 0.08 mmol), and the entire mixture was heated at 40 °C for 12 h, with vigorous stirring, under a flow of nitrogen. Toluene (20 mL) was added to the solution, and the resulting mixture was washed with aqueous NH_4Cl (2 × 20 mL) and water (2 × 20 mL). The organic components were dried over $MgSO_4$, filtered through Celite, and concentrated via rotary evaporation. The resulting solid was redissolved in hexanes, passed through an alumina plug, and concentrated via rotary evaporation. The resulting oil was added to a mixture of THF/MeOH/H_2O (15 mL/15 mL/3 mL), and the resulting mixture was stirred with K_2CO_3 (0.120 g, 0.9 mmol) for 3 h. Hexanes (30 mL) were added to the solution, and the mixture was washed with water (2 × 20 mL). The organic components were dried over $MgSO_4$, filtered through Celite, and concentrated via rotary evaporation. The resulting solid was dissolved in NEt_3 (50 mL), and the solution was sparged with nitrogen for 10 min. The degassed solution was added to a Schlenk flask containing 4-bromo-1-iodo-terafluorobenzene (0.320 g, 0.9 mmol), $Pd(PPh_3)_4$ (0.030 g, 0.03 mmol), CuI (0.020 g, 0.10 mmol), and PPh_3 (0.020 g, 0.08 mmol), and the entire mixture was heated at 30−35 °C for 12 h, with vigorous stirring, under a flow of nitrogen. Toluene (40 mL) was added to the solution, and the resulting mixture was washed with aqueous NH_4Cl (2 × 20 mL) and water (2 × 20 mL). The organic components were dried over $MgSO_4$, filtered through Celite, and concentrated via rotary evaporation. The resulting solid was absorbed onto silica gel and purified by column chromatography (hexanes) to give 0.160 g (58%, 0.32 mmol) of **3** as a yellow powder. ^1H NMR ($CDCl_3$, 400 MHz, 25 °C) δ 0.894 (3H, t), 1.3−1.4

(6H, m), 1.672 (2H, q), 2.80 (2H, t), 6.705 (1H, d), 7.019 (1H, d), 7.049 (1H, d), 7.293 (1H, d); ^{19}F NMR ($CDCl_3$, 376 MHz, 25 °C) δ −134.46 (1F, m), −136.51 (1F, m). Anal. Calcd for $C_{22}H_{17}BrF_4S_2$: C, 52.55; H, 3.42; S, 12.79. Found: C, 52.55; H, 3.59; S, 13.16. Mp 80−82 °C.

5-(1-Ethynyl-4-iodo-tetrafluorophenyl)-5′-hexyl-2,2′-bithiophene (4). Compound **3** (0.410 g, 0.82 mmol) was dissolved in toluene/Et_2O (50 mL/ 20 mL), and the solution was cooled to −78 °C. To this was added butyllithium (0.52 mL, 1.6 M in hexanes), and the solution was stirred for 20 min at −78 °C. Iodine (0.210 g, 0.83 mmol) was dissolved in Et_2O (15 mL), and this solution was then added to the stirred reaction mixture. Aqueous $Na_2S_2O_3$ was added, and the reaction mixture was allowed to warm to room temperature, with stirring, over 1 h. The mixture was washed with water (2 × 50 mL), and the organic components were dried over $MgSO_4$ and filtered through Celite, and the product was isolated via rotary evaporation to give 0.440 g (98%, 0.81 mmol) of **4** as a yellow powder. ^{1}H NMR ($CDCl_3$, 400 MHz, 25 °C) δ 0.894 (3H, t), 1.3−1.4 (6H, m), 1.663 (2H, q), 2.800 (2H, t), 6.705 (1H, d), 7.018 (1H, d), 7.047 (1H, d), 7.294 (1H, d); ^{19}F NMR ($CDCl_3$, 376 MHz, 25 °C) δ −121.59 (1F, m), −136.07 (1F, m). Anal. Calcd for $C_{22}H_{17}F_4IS_2$: C, 48.18; H, 3.12; S, 11.69. Found: C, 48.03; H, 3.40; S,11.66. Mp 89−90 °C.

2-(1-(5-Ethynyl-5′-hexyl-2,2′-bithienyl)-4-ethynyltetrafluorophenyl)-9,9-dimethyl-heptafluorosilafluorene (Si-DA). 2,2′-Dibromo-4-(1-(5-ethynyl-5′-hexyl-2,2′-bithienyl)-4-ethynyltetrafluorophenyl)-heptafluorobiphenyl (**2**) (0.100 g, 0.11 mmol) was dissolved in toluene/Et_2O (10 mL/ 2 mL), and the resulting mixture was cooled to −78 °C. To this was added butyllithium (0.14 mL, 1.6 M in hexanes), and the resulting solution was stirred for 20 min at −78 °C, after which dichlorodimethylsilane (0.1 mL) in THF (2 mL) was added, and the entire solution was allowed to warm to room temperature, with stirring, over 12 h. The resulting yellow solution was washed with water (2 × 15 mL), and the organic components were dried over $MgSO_4$, filtered through Celite, and concentrated via rotary evaporation. The product was isolated via recrystallization from hot hexanes to give 0.070 g (82%, 0.09 mmol) of **Si-DA** as a light orange powder. ^{1}H NMR ($CDCl_3$, 400 MHz, 25 °C) δ 0.623 (6H, s), 0.896 (3H, t), 1.3−1.4 (6H, m), 1.686 (2H, q), 2.805 (2H, t), 6.716 (1H, d), 7.032 (1H, d), 7.059 (1H, d), 7.315 (1H, d); ^{19}F NMR ($CDCl_3$, 376 MHz, 25 °C) δ −102.38 (1F, m), −124.31 (1F, m), −127.87 (1F, dm, J_{FF}^{45} = 147 Hz), −128.50 (1F, m), −133.96 (1F, m, J_{FF}^{45} = 147 Hz), −137.32 (2F, m), −137.83 (2F, m), −150.02 (1F, m), −152.82 (1F, m). Anal. Calcd for $C_{38}H_{23}F_{11}S_2Si$: C, 58.45; H, 2.92; S, 8.21. Found: C, 58.20; H, 2.97; S, 7.95. Mp 296−297 °C.

2-(1-(5-Ethynyl-5′-hexyl-2,2′-bithienyl)-4-ethynyltetrafluorophenyl)-9,9-diethyl-heptafluorogermafluorene (Ge-DA). 2,2′-Dibromo-4-(1-(5-ethynyl-5′-hexyl-2,2′-bithienyl)-4-ethynyltetrafluorophenyl)-heptafluorobiphenyl (**2**) (0.080 g, 0.09 mmol) was dissolved in toluene/Et_2O (10 mL/ 2 mL), and the mixture was cooled to −78 °C. To this was added butyllithium (0.14 mL, 1.6 M in hexanes), and the resulting solution was stirred for 20 min at −78 °C. In a separate Schlenk flask, dichlorodiethylgermane (0.1 mL, 0.7 mmol) was added to dry THF (2 mL), and this mixture was deoxygenated via two series of freeze/pump/thaw cycles and then added to the cooled reaction mixture. The resulting solution was warmed to room temperature, with stirring, over 8 h. The resulting yellow solution was quenched with water (2 × 15 mL), and the organic components were extracted into CH_2Cl_2 (2 × 20 mL). The combined extracts were dried over $MgSO_4$, filtered through Celite, and concentrated via rotary evaporation. The product was isolated via recrystallization from hot hexanes to give 0.045 g (83%, 0.075 mmol) of **Ge-DA** as a bright yellow powder. ^{1}H NMR ($CDCl_3$, 400 MHz, 25 °C) δ 0.896 (3H, t), 1.091 (6H, t), 1.3−1.4 (10H, m), 1.686 (2H, q), 2.805 (2H, t), 6.711 (1H, d), 7.035 (1H, d), 7.059 (1H, d), 7.315 (1H, d); ^{19}F NMR ($CDCl_3$, 376 MHz, 25 °C) δ −99.84 (1F, m), −125.48 (1F, m), −125.69 (1F, m), −126.80 (1F, dm, J_{FF}^{45} = 162 Hz), −132.99 (1F, m, J_{FF}^{45} = 162 Hz), −137.30 (2F, m), −137.85 (2F, m), −151.12 (1F, m), −152.70 (1F, m). Anal. Calcd for $C_{40}H_{27}F_{11}GeS_2$: C, 56.30; H, 3.19. Found: C, 56.20; H, 3.22. Mp 295−296 °C.

2-(1-(5-Ethynyl-5′-hexyl-2,2′-bithienyl)-4-ethynyltetrafluorophenyl)-9-ethyl-heptafluorophosphafluorene Oxide (P-DA). 2,2′-Dibromo-4-(1-(5-ethynyl-5′-hexyl-2,2′-bithienyl)-4-ethynyltetrafluorophenyl)-heptafluorobiphenyl (**2**) (0.055 g, 0.06 mmol) was dissolved in toluene/Et_2O (10 mL/ 2 mL), and the mixture was cooled to −78 °C. To this was added butyllithium (0.08 mL, 1.6 M in hexanes), and the resulting solution was stirred for 20 min at −78 °C, after which dichloroethylphosphine (0.05 mL) was added, and the entire solution was allowed to warm to room temperature over 12 h with stirring. The solvent and excess dichloroethylphospine were removed under vacuum, and the resulting orange solid was redissolved in toluene (20 mL) and washed with water (2 × 15 mL). The organic components were dried over $MgSO_4$, filtered through Celite, and concentrated via rotary evaporation. THF (20 mL) and H_2O_2 (0.2 mL, 30 wt % solution in H_2O) were added, and the resulting mixture was stirred for 4 h. Toluene (20 mL) was added, the resulting reaction mixture was washed with water (2 × 15 mL), and the organic components were dried over $MgSO_4$, filtered through Celite, and concentrated via rotary evaporation. The product was isolated via recrystallization from hot hexanes/acetone to give 0.025 g (50%, 0.03 mmol) of **P-DA** as a light orange powder. ^{1}H NMR ($CDCl_3$, 400 MHz, 25 °C) δ 0.896 (3H, t), 1.152 (3H, dt), 1.3−1.4 (6H, m), 1.675 (2H, q), 2.471 (2H, m), 2.805 (2H, t), 6.711 (1H, d), 7.037 (1H, d), 7.059 (1H, d), 7.320 (1H, d); ^{19}F NMR ($CDCl_3$, 376 MHz, 25 °C) δ −105.43 (1F, m), −118.15 (1F, m), −127.11 (1F, dm, J_{FF}^{45} = 132 Hz), −131.33 (1F, m), −132.52 (1F, m, J_{FF}^{45} = 132 Hz), −136.76 (2F, m), −137.45 (2F, m), −143.96 (1F, m), −148.53 (1F, m). ^{31}P NMR ($CDCl_3$, 161.9 MHz, 25 °C) δ 42.57 (s). MS: 799 (M^+), 727, 699. HRMS: calcd for $C_{38}H_{22}F_{11}OPS_2$ 798.067408, found 789.067320. Mp > 250 °C.

2,2′-Dibromo-4,4′-bis(1-(5-ethynyl-5′-hexyl-2,2′-bithienyl)-4-ethynyltetrafluorophenyl)-hexafluorobiphenyl (5). 2,2′-Dibromo-4,4′-ethynyl-3,3′,5,5′,6,6′-hexafluorobiphenyl (0.129 g, 0.29 mmol) and **4** (0.400 g, 0.73 mmol) were dissolved in NEt_3 (30 mL), and the solution was sparged with nitrogen for 10 min. The degassed solution was added to a Schlenk flask containing $Pd(PPh_3)_4$ (0.040 g, 0.034 mmol), CuI (0.040 g, 0.21 mmol), and PPh_3 (0.040 g, 0.15 mmol), and the entire mixture was heated at 40 °C for 12 h, with vigorous stirring, under a flow of nitrogen. Toluene was added to the solution (20 mL), and the resulting mixture was washed with aqueous NH_4Cl (2 × 20 mL) and water (2 × 20 mL). The organic components were dried over $MgSO_4$, filtered through Celite, and concentrated via rotary evaporation. The resulting solid was absorbed onto silica gel and purified by column chromatography (hexanes/toluene 100:5) to give 0.340 g (90%, 0.26 mmol) of **5** as a light orange powder. ^{1}H NMR ($CDCl_3$, 400 MHz, 25 °C) δ 0.899 (3H, t), 1.3−1.4 (6H, m), 1.690 (2H, q), 2.809 (2H, t), 6.713 (1H, d), 7.042 (1H, d), 7.068 (1H, d), 7.330 (1H, d); ^{19}F NMR ($CDCl_3$, 376 MHz, 25 °C) δ −101.66 (1F, m), −129.39 (1F, m), −136.85 (3F, m), −137.56 (2F, m). Anal. Calcd for $C_{60}H_{34}Br_2F_{14}S_4$: C, 55.05; H, 2.62; S, 9.80. Found: C, 54.77; H, 2.32; S, 10.15. Mp 186 °C dec.

2,7-Bis(1-(5-ethynyl-5′-hexyl-2,2′-bithienyl)-4-ethynyltetrafluorophenyl)-9,9-dimethyl-hexafluorosilafluorene (Si-DAD). 2,2′-Dibromo-4,4′-bis(1-(5-ethynyl-5′-hexyl-2,2′-bithienyl)-4-ethynyltetrafluorophenyl)-hexafluorobiphenyl (**5**) (0.022 g, 0.019 mmol) was dissolved in toluene/Et_2O (5 mL/ 1 mL), and the mixture was cooled to −78 °C. To this was added butyllithium (0.024 mL, 1.6 M in hexanes), and the resulting solution was stirred for 20 min at −78 °C, after which dichlorodimethylsilane (0.1 mL) in THF (1 mL) was added, and the entire solution was allowed to

warm to room temperature over 12 h with stirring. The resulting yellow solution was quenched with water (2 × 10 mL), and the organic components were extracted into toluene (2 × 10 mL). The combined extracts were dried over $MgSO_4$, filtered through Celite, and concentrated via rotary evaporation. The product was isolated via slow evaporation of hot hexanes/CH_2Cl_2 to give 0.011 g (61%, 0.009 mmol) of **Si-DAD** as an orange powder. ^{1}H NMR ($CDCl_3$, 400 MHz, 25 °C) δ 0.637 (3H, s), 0.895 (3H, t), 1.3−1.4 (6H, m), 1.685 (2H, q), 2.803 (2H, t), 6.708 (1H, d), 7.036 (1H, d), 7.0560 (1H, d), 7.316 (1H, d); ^{19}F NMR ($CDCl_3$, 376 MHz, 25 °C) δ −102.19 (1F, m), −124.28 (1F, m), −132.66 (1F, m), −137.22 (2F, m), −137.80 (2F, m). LRMS: 1207 (M^+). HRMS calcd for $C_{62}H_{40}F_{14}S_4Si$ 1206.1586, found 1206.1578. Mp 195 °C sub.

2,7-Bis(1-(5-ethynyl-5′-hexyl-2,2′-bithienyl)-4-ethynyltetrafluorophenyl)-9,9-dimethyl-hexafluorogermafluorene (Ge-DAD). 2,2′-Dibromo-4,4′-bis(1-(5-ethynyl-5′-hexyl-2,2′-bithienyl)-4-ethynyltetrafluorophenyl)-hexafluorobiphenyl (**5**) (0.080 g, 0.06 mmol) was dissolved in toluene/Et_2O (20 mL/ 5 mL), and the mixture was cooled to −78 °C. To this was added butyllithium (0.08 mL, 1.6 M in hexanes), and the resulting solution was stirred for 20 min at −78 °C. In a separate Schlenk flask, dichlorodiethylgermane (0.1 mL, 0.7 mmol) was added to dry THF (2 mL), and this mixture was deoxygenated via two series of freeze/pump/thaw cycles. The dichlorodiethylgermane solution was added to the dilithio solution at −78 °C, and the resulting reaction mixture was warmed to room temperature with stirring over 8 h. The solvent and excess dichlorodiethylgermane were removed via vacuum transfer, and the resulting yellow/orange solid was redissolved in toluene (30 mL) and washed with water (2 × 20 mL). The organic components were dried over $MgSO_4$, filtered through Celite, and concentrated via rotary evaporation. The product was isolated via recrystallization via hot hexanes/acetone to give 0.050 g (64%, 0.04 mmol) of **Ge-DAD** as an orange powder. ^{1}H NMR ($CDCl_3$, 400 MHz, 25 °C) δ 0.896 (3H, t), 1.091 (3H, t), 1.3−1.4 (8H, m), 1.686 (2H, q), 2.805 (2H, t), 6.711 (1H, d), 7.035 (1H, d), 7.059 (1H, d), 7.315 (1H, d); ^{19}F NMR ($CDCl_3$, 376 MHz, 25 °C) δ −99.61 (1F, m), −125.67 (1F, m), −131.72 (1F, m), −137.25 (2F, m), −137.82 (2F, m). Anal. Calcd for $C_{64}H_{44}F_{14}GeS_4$: C, 60.06; H, 3.47; S, 10.02. Found: C, 59.83; H, 3.27; S, 10.05. Mp 175 °C sub.

2,7-Bis(1-(5-ethynyl-5′-hexyl-2,2′-bithienyl)-4-ethynyltetrafluorophenyl)-9,9-dimethyl-hexafluorophosphafluorene Oxide (P-DAD). 2,2′-Dibromo-4,4′-bis(1-(5-ethynyl-5′-hexyl-2,2′-bithienyl)-4-ethynyltetrafluorophenyl)-hexafluorobiphenyl (**5**) (0.077 g, 0.058 mmol) was dissolved in toluene/Et_2O (20 mL/ 5 mL), and the resulting mixture was cooled to −78 °C. To this was added butyllithium (0.073 mL, 1.6 M in hexanes), and the resulting solution was stirred for 20 min at −78 °C, after which dichloroethylphosphine (0.05 mL) was added, and the entire solution was allowed to warm to room temperature over 12 h with stirring. The solvent and excess dichloroethylphosphine were removed via vacuum transfer, and the resulting yellow/orange solid was redissolved in toluene (30 mL) and washed with water (2 × 20 mL). THF (10 mL) and H_2O_2 (2 mL, 30 wt % solution in H_2O) were added, and the resulting mixture was stirred for 4 h. The reaction was quenched by washing with water (2 × 15 mL), and the organic components were dried over $MgSO_4$, filtered through Celite, and concentrated via rotary evaporation. The product was isolated via recrystallization from hot hexanes/acetone/CH_2Cl_2 to give 0.055 g (76%, 0.045 mmol) of **P-DAD** as a light orange powder. ^{1}H NMR ($CDCl_3$, 400 MHz, 25 °C) δ 0.896 (6H, t), 1.170 (3H, dt), 1.3−1.4 (12H, m), 1.667 (4H, q), 2.517 (2H, m), 2.805 (4H, t), 6.711 (2H, d), 7.035 (2H, d), 7.059 (2H, d), 7.315 (2H, d); ^{19}F NMR ($CDCl_3$, 376 MHz, 25 °C) δ −105.33 (1F, m), −118.28 (1F, m), −131.47 (1F, m), −136.70 (2F, m), −137.44 (2F, m); ^{31}P NMR ($CDCl_3$, 161.9 MHz, 25 °C) δ 41.68 (s). LRMS: 1225 (M^+). Anal. Calcd for $C_{62}H_{39}F_{14}OPS_4$: C, 60.78; H, 3.21; S, 10.47. Found: C, 60.47; H, 3.05; S, 10.38. Mp 214 −217 °C.

2,2‴-Diiodo-4,4‴-dihexyl-5,2′,2″,5‴,5′,5″-quaterthiophene (6). 3,3‴-Dihexyl-2,2′,2″,2‴,5′,5″-quaterthiophene (0.360 g, 0.72 mmol) was dissolved in THF (100 mL), to this was added butyllithium (1.0 mL, 1.6 M in hexanes), and the mixture was stirred for 1 h at room temperature. In a separate Schlenk flask iodine (0.450 g, 1.8 mmol) was dissolved in THF (20 mL), the resulting solution was added to the quaterthiophene-containing mixture, and the entire reaction mixture was stirred for 20 min. Toluene was added to the solution (40 mL), and the mixture was washed with aqueous $Na_2S_2O_3$ (2 × 40 mL) and water (2 × 40 mL). The combined organic components were dried over $MgSO_4$, filtered through Celite, and concentrated via rotary evaporation and to give 0.547 g (100%, 0.72 mmol) of **6** as yellow crystals that were used without further purification. ^{1}H NMR ($CDCl_3$, 400 MHz, 25 °C) δ 0.883 (3H, t), 1.3−1.4 (10H, m), 1.58 (2H, m), 2.872 (2H, t), 6.960 (1H, d), 7.077 (1H, s), 7.107 (1H, d).

2,2‴-Bis(1-ethynyl-4-bromo-tetrafluorophenyl)-4,4‴-dihexyl-5,2′,2″,5‴,5′,5″-quaterthiophene (7). Quaterthiophene **6** (0.547 g, 0.72 mmol) was dissolved in NEt_3 (50 mL), and to this was added trimethylsilylacetylene (0.3 mL, 2.1 mmol). The entire solution was sparged with nitrogen for 10 min and was then added to a Schlenk flask containing $PdCl_2(PPh_3)_2$ (0.040 g, 0.06 mmol), CuI (0.040 g, 0.21 mmol), and PPh_3 (0.040 g, 0.15 mmol), and the entire mixture was heated at 40 °C for 12 h, with vigorous stirring, under a flow of nitrogen. Toluene was added to the solution (30 mL), and the resulting mixture was washed with aqueous NH_4Cl (2 × 20 mL) and water (2 × 20 mL). The organic components were dried over $MgSO_4$, filtered through Celite, and concentrated via rotary evaporation. The resulting solid was dissolved in a mixture of THF/MeOH/H_2O (20 mL/20 mL/5 mL) and stirred with K_2CO_3 (0.184 g, 1.3 mmol) for 3 h. Toluene was added to the solution (40 mL), and the mixture was washed with water (2 × 20 mL). The organic components were dried over $MgSO_4$, filtered through Celite, and concentrated via rotary evaporation. The resulting solid was dissolved in NEt_3 (50 mL), and the resulting solution was sparged with nitrogen for 10 min. The degassed solution was added to a Schlenk flask containing 4-bromo-1-iodo-terafluorobenzene (1.00 g, 2.80 mmol), $PdCl_2(PPh_3)_2$ (0.040 g, 0.06 mmol), CuI (0.030 g, 0.16 mmol), and PPh_3 (0.030 g, 0.11 mmol), and the entire mixture was heated at 30−35 °C for 12 h, with vigorous stirring, under a flow of nitrogen. Toluene was added to the solution (40 mL), and the mixture was washed with aqueous NH_4Cl (2 × 20 mL) and water (2 × 20 mL). The organic components were dried over $MgSO_4$, filtered through Celite, and concentrated via rotary evaporation. The resulting solid was absorbed onto silica gel and purified by column chromatography (hexanes:toluene) to give 0.275 g (39%, 0.28 mmol) of **7** as a red powder. ^{1}H NMR ($CDCl_3$, 400 MHz, 25 °C) δ 0.890 (3H, t), 1.3−1.4 (6H, m), 1.670 (2H, q), 2.77 (2H, t), 7.106 (1H, d), 7.172 (1H, d), 7.260 (1H, d); ^{19}F NMR ($CDCl_3$, 376 MHz, 25 °C) δ −134.48 (1F, m), −136.43 (1F, m). Anal. Calcd for $C_{44}H_{32}Br_2F_8S_4$: C, 52.81; H, 3.22; S, 12.82. Found: C, 52.86; H, 3.29; S, 12.97. Mp 180−181 °C.

2,2‴-Bis(1-ethynyl-4-iodo-tetrafluorophenyl)-4,4‴-dihexyl-5,-2′,2″,5‴,5′,5″-quaterthiophene (8). Compound **7** (0.066 g, 0.066 mmol) was dissolved in THF (50 mL), and the resulting solution was cooled to −78 °C. To this was added butyllithium (0.9 mL, 1.6 M in hexanes), and the resulting solution was stirred for 20 min at −78 °C. Iodine (0.35 g, 0.14 mmol) was dissolved in THF (10 mL), and the iodine solution was then added to the stirred reaction mixture. Aqueous $Na_2S_2O_3$ was added, and the reaction mixture was allowed to warm to room temperature with stirring over 1 h. Toluene was added to the solution (40 mL), and the resulting mixture was washed with water (2 × 50 mL). The organic components were dried over $MgSO_4$ and filtered through Celite, and the product was isolated via rotary evaporation to give 0.072 g (94%, 0.065 mmol) of **8** as a red powder. ^{1}H NMR ($CDCl_3$, 400 MHz, 25 °C) δ 0.890 (3H, t), 1.3−1.4 (6H, m), 1.670 (2H, q), 2.77 (2H, t), 7.106 (1H, d), 7.172 (1H, d), 7.260 (1H, d);

^{19}F NMR ($CDCl_3$, 376 MHz, 25 °C) δ −121.51 (1F, m), −135.99 (1F, m). Anal. Calcd for $C_{44}H_{32}I_2F_8I_2S_4$: C, 48.27; H, 2.95; S, 11.72. Found: C, 48.26; H, 2.95; S, 11.78. Mp 188−189 °C.

2,2‴-Bis(1-ethynyl-4-(2,2′-dibromo-4-ethynyl-heptafluororbiphenyl)-tetrafluorophenyl)-4,4‴-dihexyl-5,2′,2″,5‴,5′,5″-quaterthiophene (9). 2,2′-Dibromo-4-ethynyl-3,3′,4′,5,5′,6,6′-heptafluorobiphenyl (0.060 g, 0.13 mmol) and **8** (0.035 g, 0.032 mmol) were dissolved in NEt_3 (50 mL), and the solution was sparged with nitrogen for 10 min. The degassed solution was added to a Schlenk flask containing $Pd(PPh_3)_4$ (0.005 g, 0.007 mmol), CuI (0.005 g, 0.03 mmol), and PPh_3 (0.010 g, 0.04 mmol), and the entire mixture was heated at 40 °C for 12 h, with vigorous stirring, under a flow of nitrogen. Toluene (40 mL) was added to the solution, and the resulting mixture was washed with aqueous NH_4Cl (2 × 30 mL) and water (2 × 30 mL). The organic components were dried over $MgSO_4$, filtered through Celite, and concentrated via rotary evaporation. The resulting solid was absorbed onto silica gel and purified by column chromatography (hexanes/toluene 5:1) to give 0.035 g (67%, 0.02 mmol) of **9** as a brick red powder. ^{1}H NMR ($CDCl_3$, 400 MHz, 25 °C) δ 0.890 (3H, t), 1.3−1.4 (6H, m), 1.670 (2H, q), 2.77 (2H, t), 7.106 (1H, d), 7.172 (1H, d), 7.260 (1H, d); ^{19}F NMR ($CDCl_3$, 376 MHz, 25 °C) δ −101.59 (1F, m), −128.40 (1F, m), −129.50 (1F, m), −135.27 (1F, m), −136.85 (3F, m), −137.56 (2F, m), −150.71 (1F, m), −154.87 (1F, m). Anal. Calcd for $C_{72}H_{32}Br_4F_{22}S_4$: C, 49.05; H, 1.83. Found: C, 49.00; H, 1.47. Mp 276−278 °C.

2,2‴-Bis(1-ethynyl-4-(2-ethynyl-9,9-diethyl-heptafluorogermafluorene)-tetrafluorophenyl)-4,4‴-dihexyl-5,2′,2″,5‴,5′,5″-quaterthiophene (Ge-ADA). 2,2‴-Bis(1-ethynyl-4-(2,2′-dibromo-4-ethynyl-heptafluororbiphenyl)-quaterfluorophenyl)-4,4‴-dihexyl-5,2′,2″,5‴,5′,5″-quaterthiophene (**9**) (0.045 g, 0.025 mmol) was dissolved in toluene/THF (10 mL/10 mL), and the mixture was cooled to −78 °C. To this was added butyllithium (0.06 mL, 1.6 M in hexanes), and the resulting brown/yellow solution was stirred for 20 min at −78 °C. In a separate Schlenk flask, dichlorodiethylgermane (0.1 mL, 0.7 mmol) was added to dry THF (2 mL), and this mixture was deoxygenated via two series of freeze/pump/thaw cycles. The dichlorodiethylgermane solution was added to the dilithio solution at −78 °C, and the resulting solution was warmed to room temperature with stirring over 8 h. The resulting red solution was quenched with water (2 × 15 mL), and the organic components were extracted into toluene (2 × 20 mL). The combined extracts were dried over $MgSO_4$, filtered through Celite, and concentrated via rotary evaporation. The product was isolated via recrystallization from hot CH_2Cl_2 to give 0.030 g (72%, 0.018 mmol) of Ge-ADA as a bright red powder. ^{1}H NMR ($CDCl_3$, 400 MHz, 25 °C) δ 0.905 (3H, t), 1.094 (6H, t), 1.3−1.4 (10H, m), 1.680 (2H, q), 2.780 (2H, t), 7.117 (1H, d), 7.182 (1H, d), 7.281 (1H, d); ^{19}F NMR ($CDCl_3$, 376 MHz, 25 °C) δ −99.85 (1F, m), −125.48 (1F, m), −125.71 (1F, m), −126.83 (1F, dm, J_{FF}^{45} = 173 Hz), −133.02 (1F, m, J_{FF}^{45} = 173 Hz), −137.25 (2F, m), −137.85 (2F, m), −151.15 (1F, m), −152.70 (1F, m). Anal. Calcd for $C_{80}H_{52}F_{22}Ge_2S_4$: C, 56.36; H, 3.07. Found: C, 55.48; H, 3.02. Mp > 300 °C.

Solar Cell Device Construction and Measurement. Sputtered ITO-coated (150 nm, 20 Ω m^{-1}) glass substrates were obtained from Thin Film Devices, Inc. The substrates were subjected to ultrasonication for 20 min in acetone, and then 2% Helmanex soap in water for 20 min, followed by extensive rinsing with deionized water and ultrasonication in deionized water and then 2-propanol. The substrates were then dried under a stream of nitrogen before treatment for 10 min in an oxygen plasma at 300 mTorr (1 Torr = 133.28 Pa) at high power. PEDOT:PSS in water (Baytron-P) was filtered through a 0.45 μm filter and spin-coated onto the ITO surface at 4000 rpm for 60 s and baked for 1 h at 125 °C, affording a 30 nm layer. All procedures after this point were performed in an inert-atmosphere glovebox. Solutions of P3HT and DA compounds were prepared separately in $CHCl_3$ (10 mg mL^{-1}). Immediately prior to deposition, the solutions were passed though a 0.2 μm polytetrafluoroethylene syringe filter. For a 1:1 wt % P3HT/DA compound device, equal amounts of each solution were combined. The blend solution was applied to the substrate and spun at 1000 rpm for 60 s. A small portion of the organic layer was removed with tweezers to allow contact with the ITO. The substrates were then placed in a resistive-heating evaporation chamber and held under vacuum (10^{-7} torr) for 4 h before evaporating 100 nm of Al through a shadow mask at a rate of 0.1−0.5 nms^{-1} while rotating the substrates at approximately 1 Hz to ensure even electrode deposition. The configuration of the shadow mask afforded eight independent devices on each substrate and one rectangular pad to connect the Al to the ITO substrate. Devices were left to cool to room temperature before further processing. Testing of the devices was performed under an argon atmosphere with an oriel xenon arc lamp with an AM 1.5G solar filter. Current−voltage behavior was measured with a Keithly 236 SMU instrument. Reported efficiencies are the average from 8 independent measurements made on one spin-coated device.

Acknowledgment. This work was supported by the National Science Foundation under research grant CHE0314709 and the DuPont Center for Collaborative Research and Education. Photovoltaic device fabrication and characterization was supported by the DOE-BES Plastic Electronics Program at Lawrence Berkeley National Laboratories. Work at the Molecular Foundry was supported by the Office of Science, Office of Basic Energy Sciences, of the U.S. Department of Energy under Contract No. DE-AC02-05CH11231. The authors would like to thank A. D'Aléo for low-temperature fluorescence data and numerous insightful discussions.

Supporting Information Available: NMR spectra for all new compounds, tables of atom coordinates and absolute energies for the theoretical calculations, and additional photovoltaic device performance data. This material is available free of charge via the Internet at http://pubs.acs.org.